UCRL-17169

University of California
Ernest O. Lawrence Radiation Laboratory

KINETICS OF FORMATION OF XENON FLUORIDES

TWO-WEEK LOAN COPY

This is a Library Circulating Copy which may be borrowed for two weeks. For a personal retention copy, call Tech. Info. Division, Ext. 5545

Berkeley, California

DISCLAIMER

This document was prepared as an account of work sponsored by the United States Government. While this document is believed to contain correct information, neither the United States Government nor any agency thereof, nor the Regents of the University of California, nor any of their employees, makes any warranty, express or implied, or assumes any legal responsibility for the accuracy, completeness, or usefulness of any information, apparatus, product, or process disclosed, or represents that its use would not infringe privately owned rights. Reference herein to any specific commercial product, process, or service by its trade name, trademark, manufacturer, or otherwise, does not necessarily constitute or imply its endorsement, recommendation, or favoring by the United States Government or any agency thereof, or the Regents of the University of California. The views and opinions of authors expressed herein do not necessarily state or reflect those of the United States Government or any agency thereof or the Regents of the University of California.

Special
Thesis

UCRL-17169

UNIVERSITY OF CALIFORNIA

Lawrence Radiation Laboratory
Berkeley, California

AEC Contract No. W-7405-eng-48

KINETICS OF FORMATION OF XENON FLUORIDES

Clayton Fred Weaver

(Ph.D. Thesis)

September 1966

KINETICS OF FORMATION OF XENON FLUORIDES

Clayton Fred Weaver

Inorganic Materials Research Division, Lawrence Radiation Laboratory,
Department of Chemistry, University of California
Berkeley, California

September 1966

ABSTRACT

The temperature dependence of the near ultraviolet region of the absorption spectra of F_2 and XeF_2 was determined to 400°C in fluorinated nickel cells with calcium fluoride windows. That of XeF_4 was determined to 250°C. This spectral information was used to study the kinetics of the formation of XeF_2 and XeF_4 in the same temperature regions and in the same temperature regions and in the same nickel cells.

Experimental conditions were chosen to cause the reactions to terminate at XeF_2 or XeF_4 as desired. With a total pressure of reactants in the 10 to 40 mm range and Xe to F_2 ratios of 10 or more the reaction $Xe + F_2 \rightarrow XeF_2$ occurred. Under these conditions the reaction was zero order in Xe and first order in F_2 over the temperature range 190 to 400°C. With total reactant pressures of 10 to 20 mm and F_2 to Xe ratios of 16 or more the reaction $Xe + 2F_2 \rightarrow XeF_4$ occurred with XeF_2 as an intermediate. Under these conditions in the temperature range 190 to 250°C the formation of XeF_2 was zero order in F_2 and first order in Xe, just the opposite of the results above. The formation of XeF_4 was zero order in F_2 and first order in XeF_2.

In all cases studied the reaction rates were independent of the concentration of inert gas which was argon but were reduced by an increased volume to surface ratio. Hence the reactions were heterogeneous, even though they were very reproducible. The activation energies were uniformly

low ranging from 12.8 to 15.7 kcal/mole in this study compared with 10.2 kcal/mole reported by Baker and Fox, who studied the formation of XeF_2 on nickel wires with the higher Xe and F_2 pressures of 300 mm each (Nature 204, 466 (1964)). It was found that the manometer oil, $Cl(CF_2CFCl)_5Cl$, acted as a poison for the fluorinated nickel catalyst reducing all observed reaction rates by more than an order of magnitude.

A mechanism involving adsorption and dissociation of F_2 on the NiF_2 surface is proposed. It yields the zero order reaction rate dependence on both reactants observed by Baker and Fox, each of the three rate expressions obtained experimentally in this study, and predicts that a rate expression first order in both Xe and F_2 should be observed at very low pressures of both Xe and F_2. It also indicates that the observed decrease in the activation energy of the rate constants with increased F_2 pressures is to be expected.

TABLE OF CONTENTS

	Page
Introduction	1
Apparatus	14
Materials	21
Spectra	22
Fluorine	22
Xenon Difluoride	29
Xenon Tetrafluoride	32
Fluorine: Theoretical Analysis	35
Kinetics Procedure	36
Mechanical Operation	36
Absence of Xenon Hexafluoride	38
General Equations	39
Discussion of Problems	41
The Reaction of Xenon and Fluorine in Excess Xenon	45
The Reaction $Xe + F_2 \rightleftharpoons XeF_2$: General Considerations	45
Variable Dependence	46
The Reaction of Xenon and Fluorine in Excess Fluorine	53
The Reaction $Xe + 2F_2 \rightleftharpoons XeF_4$: General Considerations	53
Variable Dependence for $Xe + F_2 \rightleftharpoons XeF_2$	55
The Reaction $XeF_2 + F_2 \rightleftharpoons XeF_4$	58

Contents (Conts.)

	Page
Poisoning of the Catalyst	60
Equilibrium Constants	61
Discussion	63
Integrated Rate Expressions	63
Mechanism	65
Miscellaneous	69
Acknowledgements	71
Appendix	72
Bibliography	103

LIST OF TABLES

Table Number	Title	Page
I.	Equilibrium Constants for the Xenon-Fluorine System	2
II.	Enthalpy and Entropy of Formation of the Xenon Fluoride Compounds	5
III.	Bond Energies of Fluorine and the Xenon Fluorides	7
IV.	Thermal Excitation of Fluorine	24
V.	Absorption Coefficients of Fluorine	26
VI.	Beer's Law Data for Fluorine at 2918 Å	28
VII.	Absorption Coefficients of Xenon Difluoride	31
VIII.	Absorption Coefficients of Xenon Tetrafluoride	34
IX.	Definition of Symbols	40
IXa.	Rate Constants	46
X.	Rate Constants	50
XI.	Activation Energies and Pre-exponential Factors	52
XII.	The Rate Constant k_4	59
XIII.	Equilibrium Constant Data at 250°C.	62
XIV.	Definition of Symbols	66
XV.	Derived Rate Expressions	67

LIST OF FIGURES

Figure Number	Title	Page
1.	Equilibrium Constants for the Xenon Fluorides	3,4
2.	Vapor Pressures for the Xenon Fluorides	8
3.	Spectra at 23°C.	9
4.	Block Diagram of Apparatus	15
5.	Response Curves of Apparatus	17
6.	Typical Response Curve for the Reaction of Xenon and Fluorine in Excess Xenon	19
7.	Potential Energy Diagram for Fluorine	23
8.	Fluorine Spectra	25
9.	Beer's Law Plot for Fluorine	27
10.	Xenon Difluoride Spectra	30
11.	Xenon Tetrafluoride Spectra	33
12.	Typical Pair of Response Curves for the Reaction of Xenon and Fluorine in Excess Fluorine	37,37a
13.	Typical Set of Concentration Curves for the Reaction of Xenon and Fluorine in Excess Xenon	47
14.	Typical Fluorine Behavior for the Reaction of Xenon and Fluorine in Excess Xenon	48

Figures (Contd.)

Figure Number	Title	Page
15.	Arrhenius Plots for the Rate Constants	51
16.	Typical Set of Concentration Curves for the Reaction of Xenon and Fluorine in Excess Fluorine	56
17.	Typical Xenon Behavior for the Reaction of Xenon and Fluorine in Excess Fluorine	57

INTRODUCTION

The problem was to determine the kinetics of the formation of xenon difluoride and xenon tetrafluoride by observing the change in absorption of near ultraviolet light. To accomplish the kinetics study it was necessary to make a prior investigation of the temperature dependence of the spectra of fluorine, xenon difluoride and xenon tetrafluoride in the near ultraviolet region.

Except for very recent work a comprehensive review of fluorine-xenon chemistry may be found in references 1 and 2. The portion of the literature pertinent to this work is outlined here. Further details are discussed in the appropriate sections.

The reactions $Xe + F_2 \rightleftharpoons XeF_2$[1,3], $XeF_2 + F_2 \rightleftharpoons XeF_4$[1,3-6] and $XeF_4 + F_2 \rightleftharpoons XeF_6$[1,6] have been reported as well as the equilibrium constants[1,7] shown in Table I. These equilibrium constants were also shown in Figures 1a and 1b since several of the temperatures used in the kinetic studies were between those listed in Table I. It should be noted that the constants from references 1 and 7 are more reliable than preliminary ones reported by the same authors.[8] Values of ΔH^o and ΔS^o calculated from these equilibrium constants using the relations $\Delta F^o = -RT\ln K$, $\ln(K_2/K_1) = (\Delta H^o/R)(1/T_1-1/T_2)$, and $\Delta S^o = (\Delta H^o-\Delta F^o)/T$ agree reasonably well with those determined by other means as shown in Table II. Hence, the equilibrium constants are considered reliable. However,

Table I

Equilibrium Constants for the Xenon-Fluorine System[a]

Reaction	Temperature °K				
	298.15	523.15	573.15	623.15	673.15
$Xe + F_2 = XeF_2$	1.23×10^{13}	8.79×10^{4}	1.02×10^{4}	1.67×10^{3}	3.59×10^{2}
$XeF_2 + F_2 = XeF_4$	1.37×10^{11}	1.43×10^{3}	1.55×10^{2}	27.2	4.86
$XeF_4 + F_2 = XeF_6$	8.6×10^{5}	0.944	0.211	0.0558	0.0182

[a] Units are in atmospheres. This table was taken directly from J. G. Malm, H. Selig, J. Jortner, and S. A. Rice, The Chemistry of Xenon, Chem. Rev. 65, 199 (1965).

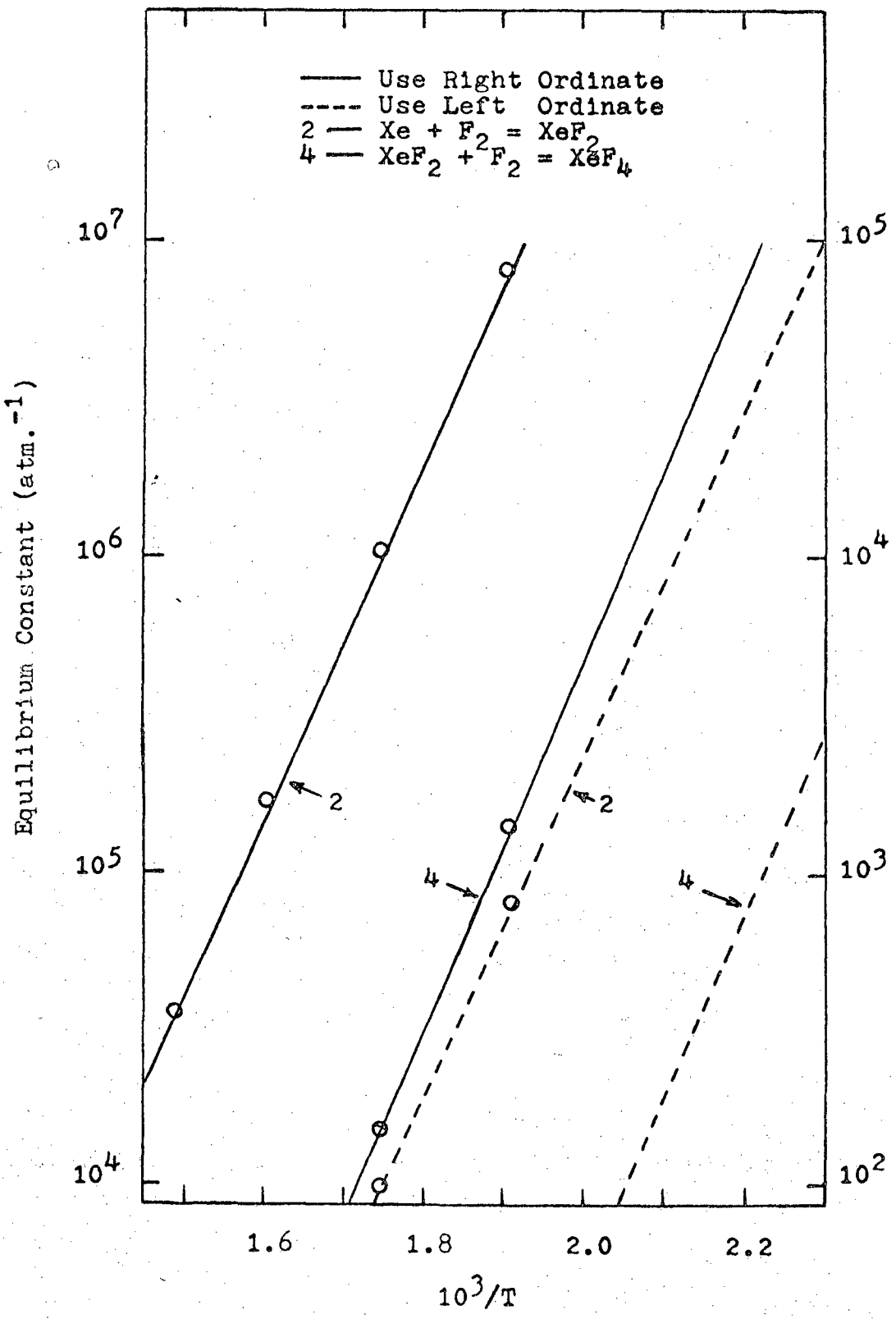

Figure 1a. Equilibrium Constants for the Xenon Fluorides

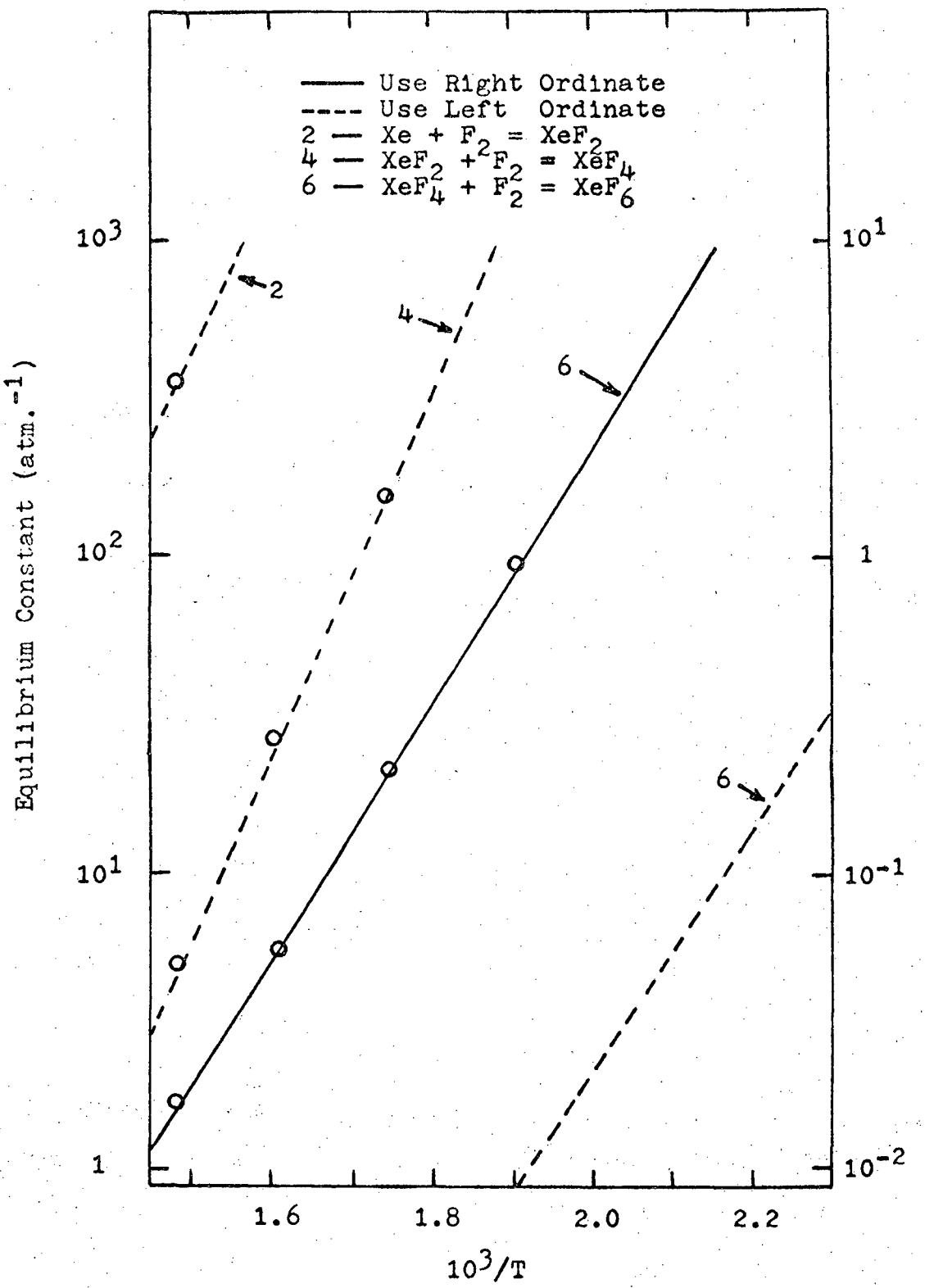

Figure 1b. Equilibrium Constants for the Xenon Fluorides

Table II

Enthalpy and Entropy of Formation of the Xenon Fluoride Compounds

	XeF_2	XeF_4	XeF_6
$\Delta H^{\circ}_{f(g)}$	-26.8[a]	-52.6[a]	-71.9[a]
$\left(\frac{\text{Kcal.}}{\text{mole.}}\right)$	-27[c]	-55[b]	-79[b]
		-57.6[e]	-82.9[e]
		-48[e]	-83[c]
		-52[c]	
$\Delta S^{\circ}_{f(g)}$	-28.5[a]	-63.8[a]	-101[a]
$\left(\frac{\text{cal.}}{\text{mole.deg.}}\right)$	-26.96[d]		

a. Calculated from equilibrium constants in Table I.

b. L. Stein and F.L. Plurien, Noble-Gas Compounds, University of Chicago Press, Chicago, Ill., 1963, p. 144.

c. Calculated from bond energies in Table III.

d. B. Weinstock, E. E. Weaver, and C. P. Knop, Noble-Gas Compounds, University of Chicago Press, Chicago, Ill., 1963, p. 50.

e. J. G. Malm, H. Selig, J. Jortner, and S. A. Rice, Chem. Rev. 65, 199 (1965).

to minimize dependence on these numbers they were used only to determine the appropriate pressures to cause the reactions $Xe + F_2 \rightleftharpoons XeF_2$ and $Xe + 2F_2 \rightleftharpoons XeF_4$ to go to completion. Bond energies of these materials, used in calculating some of the numbers in Table II, are shown in Table III.

The temperature relations of the vapor pressures[9] of xenon difluoride and of xenon tetrafluoride are shown in Figure 2. These, of course, fix the upper limits for the pressures of the xenon compounds in the spectral and kinetic studies.

Information is available for the ultraviolet absorption of fluorine,[10-14] xenon difluoride,[15-17] and xenon tetrafluoride[15,16,18] at room temperature. A graphical summary of this information may be seen in Figure 3. Xenon is transparent in the near ultraviolet region. No quantitative data are available for the absorption of xenon hexafluoride, but it has been described[1,19] as strong at 3300 Å with a half width of 580 Å and very intense below 2750 Å. A very limited amount of data on the temperature dependence of the absorption coefficients*

---

* Absorption coefficient is defined in this report as $\ln(I^0/I)/LC$. I^0 = intensity with vacuum, I = intensity with C, C = concentration in moles/cc, L = length in cm, and ln = natural logarithm.

Table III

Bond Energies of Fluorine and the Xenon Fluorides

Bond Energy (kcal./mole)	Reaction
48[a]	$XeF_4 = XeF_3 + F$
15[a]	$XeF_3 = XeF_2 + F$
54[a]	$XeF_2 = XeF + F$
11[a]	$XeF = Xe + F$
37.7[b]	$F_2 = F + F$
31.3[c] (average)	$XeF_2 = Xe + 2F$
30[d] (average)	$XeF_4 = Xe + 4F$
32.8[c] (average)	$XeF_4 = Xe + 4F$
32.3[c] (average)	$XeF_6 = Xe + 6F$

[a] H. S. Johnston and R. Woolfolk, J. Chem. Phys. 41, 269-273 (1964).

[b] R. N. Doescher, J. Chem. Phys. 20, 330 (1952).

[c] J. G. Malm, H. Selig, J. Jortner, and S. A. Rice, Chem. Rev. 65, 199 (1965).

[d] S. R. Gunn and S. M. Williamson, Noble-Gas Compounds, University of Chicago Press, Chicago, Ill., 1963, p. 133.

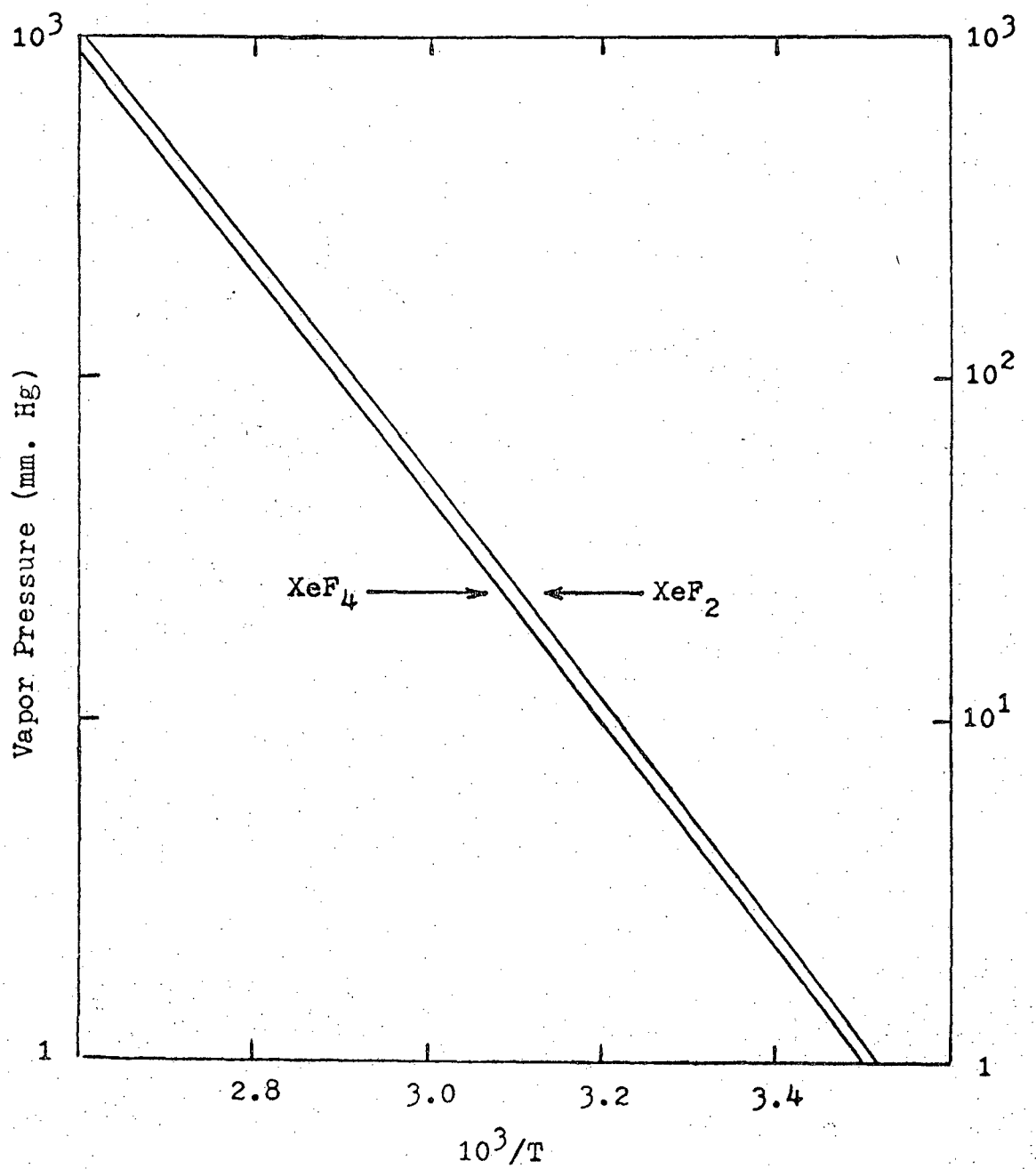

Figure 2. Vapor Pressures of the Xenon Fluorides

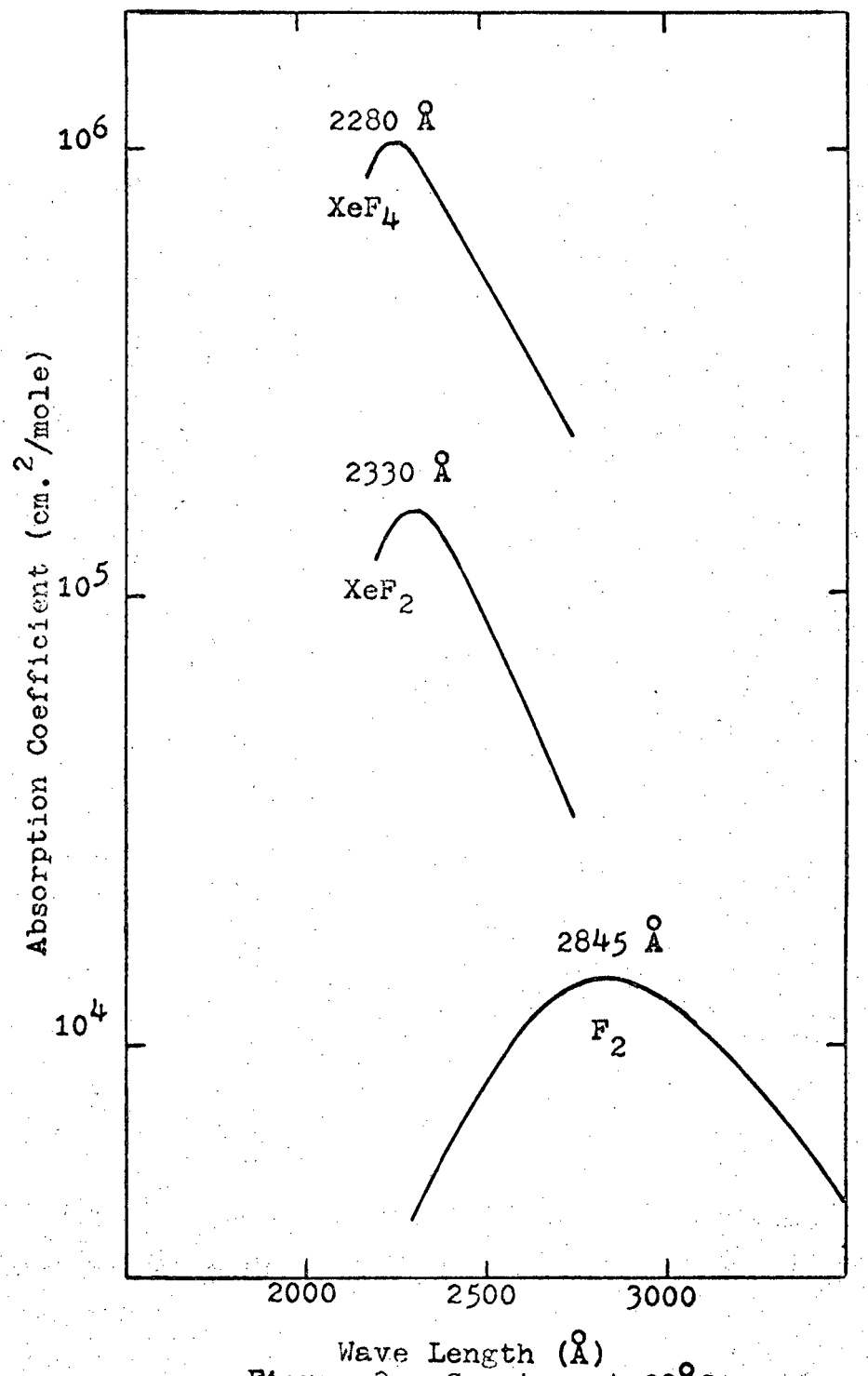

Figure 3. Spectra at 23°C

of fluorine[14] and xenon difluoride[16] are also available. Infrared spectra for xenon difluoride[3] and xenon tetrafluoride[20] and Raman spectra for xenon tetrafluoride[20] and fluorine[21-23] are available. The geometries[20,24] of these molecules are known and the frequencies assigned[24] to the corresponding normal modes. The relation between these frequencies and geometries and the temperature dependence of the near ultraviolet spectra is discussed on pp. 22-35. The free radical XeF has been reported[1,25-27] with absorption bands at 3300 Å and 2500 Å. Its bond energy has been estimated[28] to be 11 kcal./mole and from this information it was considered to be an important species in shock tube experiments.[29]

Very qualitative kinetic information has been given in synthesis studies in nickel containers. Xenon difluoride has been synthesized[1,3,30] in a loop by circulating fluorine and xenon through a section heated to 400°C and freezing the product at -50°C in another portion. The reaction required eight hours to reach completion. However, since the reactants were in the hot zone for a very small fraction of the time the reaction rate must have been far faster than indicated. The reactions $Xe + F_2 \rightleftharpoons XeF_2$, $Xe + 2F_2 \rightleftharpoons XeF_4$ and $XeF_2 + F_2 \rightleftharpoons XeF_4$ were monitored in this loop by following the infrared absorption. These studies indicated that the reaction rate of xenon and fluorine increased with temperature,

partial pressure of fluorine, and partial pressure of xenon. They also indicated that the reaction rate of xenon difluoride and fluorine increased with temperature, with partial pressure of fluorine and with partial pressure of xenon difluoride. It was further observed that in mixtures of xenon and fluorine xenon difluoride was first formed and then the xenon tetrafluoride appeared. This indicates that xenon difluoride is not by passed in the formation of the tetrafluoride. This conclusion is strength- by the observation mentioned above that freezing out xenon difluoride at -50°C immediately after it is formed prevents the production of xenon tetrafluoride.

Xenon tetrafluoride has been synthesized[4] from a mixture of 1.06 atmospheres of xenon and 9.6 atmospheres of fluorine (pressures measured at room temperature) by heating to 400°C. The reaction was complete in one hour. At the somewhat lower pressures of 1 atmosphere of xenon and 5 atmospheres of fluorine (pressures measured at 400°C) the reaction was also complete in one hour.[1,5,6] In a flow method with a 4:1 molar ratio of fluorine to xenon in a nickel tube at 300°C and a residence time of one minute in the hot zone the yield of xenon tetrafluoride was 100 percent.[1,31]

Xenon hexafluoride forms from a mixture of about 3 atm. xenon and about 60 atm. of fluorine (pressures measured at reaction temperature) at 300°C in 16 hours.[6]

Other workers using pressures of 25 to 500 atmospheres at 227°C produced xenon hexafluoride in 1 to ten days.[32]

The only reported quantitative kinetics study[33] was made with a cold silica vessel containing electrically heated wires of nickel, copper, aluminum, and platinum. The reactions were followed by monitoring the pressure with an all-metal bellows manometer. The fluorine pressure was about 300 mm Hg with initial fluorine to xenon ratios in the range 0.8 to 2.0. The temperature range was 180 to 400°C. The reaction was of zero order until about half of the material had reacted if the wall temperature was -78°C. Under these conditions the activation energy was 10.4 Kcal./mole, and the pre-exponential factor was about 10^{21} molecules $sec.^{-1}$ cm^{-2}, a number which is comparible to the collision frequency of the xenon with the nickel wire. Rates were lower and zero order conditions held for a much smaller extent of the reaction if the vessel wall was at 0°C suggesting product interference. Heating xenon and fluorine in the silica vessel without hot metal produced no reaction at all. Repeating the hot wire experiments with copper, aluminum, and platinum produced no reaction in the range 180 to 400°C. At slightly higher temperatures xenon and fluorine reacted if copper or aluminum was used. At 510°C the platinum reacted with fluorine. It was concluded that the reaction between xenon and fluorine was catalyzed by

a nickel surface and to a lesser extent by copper and aluminum surfaces. These results indicate that the rate of homogeneous xenon-fluorine reactions in the temperature range 180 to 400°C was undetectably small.

APPARATUS

A block diagram of the apparatus used may be seen in Figure 4. The hot cell consisted of a fluorinated nickel tube 146 cm long and 1.59 cm inside diameter with single crystal CaF_2[34] windows sealed to the nickel with Viton[35] (also called Fluorel Rubber) o-rings. The important properties of calcium fluoride for this study were resistance to fluorine and fluorides, resistance to atmosphere, stability at elevated temperatures, and transmission of the near ultraviolet radiation. The tube was heated with three 1000 watt resistance heaters, one near the midpoint and one at each end near the windows. This unit was used to 250°C. above which three heating units were insufficient to produce a reasonably flat temperature distribution. For the higher temperatures a cell using six 576 watt heating elements was used. This cell also was 146 cm long but its inside diameter was 6.28 cm allowing an evaluation of the effect of surface to volume ratio. The window region of this furnace could be water or air cooled. These furnaces, insulated with foam mica, required several hours to reach thermal steady state. Primarily because of this high heat capacity the temperature was sufficiently stable over the period of one hour or less required for the reactions that no temperature regulating system was necessary.

The ultraviolet source was a Bausch & Lomb air cooled deuterium arc lamp with a fused quartz condenser system.[36]

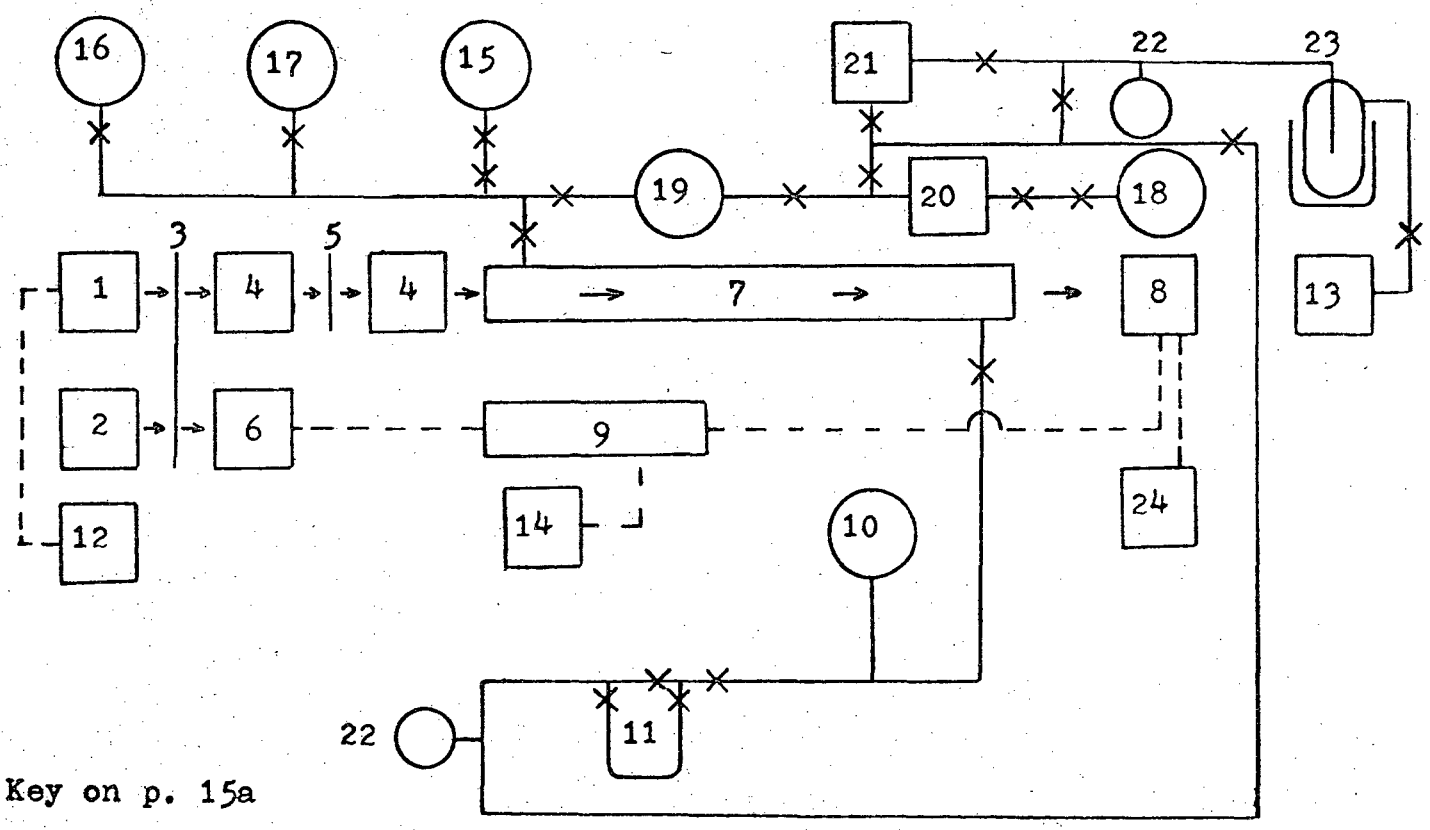

Key on p. 15a

Figure 4. Block Diagram of Apparatus

Key for Figure 4

1. Ultraviolet Source
2. Tungsten Light
3. Chopper
4. Monochromator
5. Shutter
6. Solar Cell
7. Hot Cell
8. 1P28
9. Lock-in Amplifier
10. Helicoid Gage
11. Manometer
12. Power Supply (0.8 ampere)
13. Vacuum Pump
14. Recorder
15. Mixing Tank (1,750 cm^3)
16. Commercial Argon
17. Commercial Xenon
18. Commercial Fluorine
19. Purified Fluorine
20. Cold NaF Trap
21. Hot (100°C) NaCl Trap
22. Thermocouple Gauge
23. Pyrex Trap in Liquid N_2
24. Power Supply (1000 volt)

→ Light Path

—— Gas Line

--- Electrical Line

X Valve

This was followed by a double monochromator consisting of two Bausch & Lomb 2700 grooves per mm gratings[36] necessary to reduce the scattering from a single unit. Scattering from a single unit was noticed by a distinct wave length independent tail on the response curve (Figure 5, curve C) at wave lengths near 2300 Å where the scattered light gave a more intense response than the frequency passed by the grating. This tail was extremely pronounced if the 1P28 was replaced by a 931A multiplier phototube[37] which is less sensitive to the higher frequencies passed by the grating but responsive to the lower frequencies from scattering (Figure 5, curve D). The indications of reduced scattering with the double monochromator unit were the narrowing of the response curve, the absence of the scattering tail, and the complete absence of response with misaligned gratings. An additional advantage of the double monochromator was the reduction of the reciprocal linear dispersion from 32 Å/mm to 16 Å/mm. The monochromator unit was calibrated by locating the easily assignable Hg lines[38] at 2536.52 Å, 2967.28 Å, 2893.60 Å and 3341.48 Å. The source used was a low pressure General Electric Germicidal Lamp No. G4T4. It was found that 18 Å should be added to the monochromator readings. This explains why most of the wave lengths tabulated later in this report end in the unlikely numbers 18 and 68. The monochromator output was focused by a Bausch & Lomb Quartz Fluorite

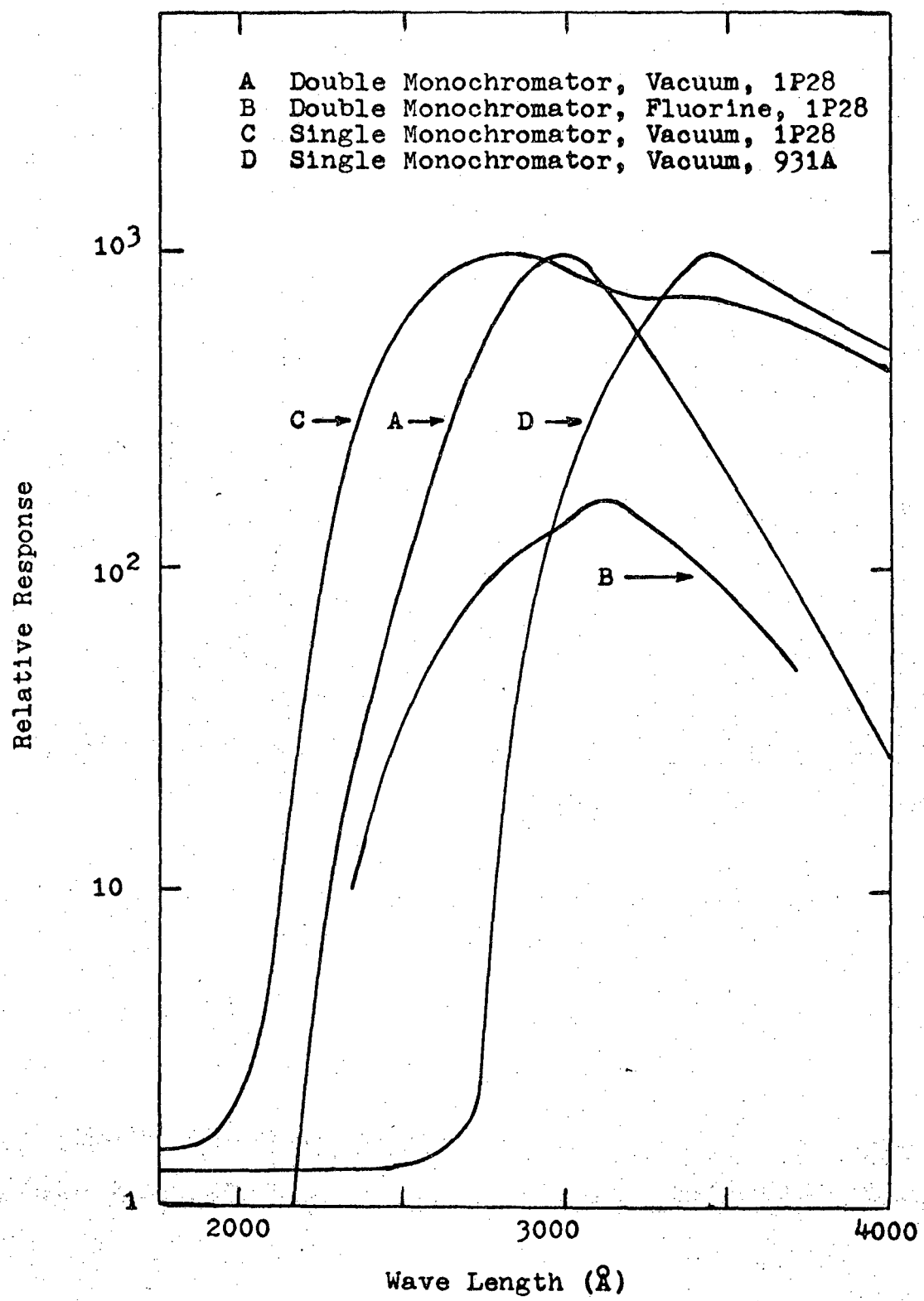

Figure 5. Response Curves of Apparatus

Achromatic condenser.[36]

The detector was a 1P28 multiplier phototube[39] operated at 1000 volts. The signal was amplified by a JB-5 Lock-in Amplifier manufactured by the Princeton Applied Research Corporation. The AC signal was generated by chopping the light beam at 26 2/3 pulses per second. This was a convenient rate which avoided the sluggish low frequency range of the Lock-in Amplifier and 60 cycle multiples. An external reference signal was generated by chopping a tungsten lamp light beam which impinged on a silicon Solar Cell (S1020GE8PL). The same unit was used to chop the reference light and the ultraviolet radiation thus insuring that these frequencies were always identical. The amplified signal was recorded by a Rectiriter rectilinear recording milliammeter manufactured by Texas Instruments Incorporated. The response curve for this system may be seen in Figure 5. Curve A represents the evacuated system. Curve B represents the system with 20mm of fluorine. The shoulder near 2500 Å drops out as the xenon fluorides are produced by reaction in the cell. The signal to noise ratio for this system was about ten to one in the typical case (Figure 6) and frequently much higher.

The pressures were measured with a Monel Helicoid gage manufactured by the American Chain & Cable Company and by a manometer constructed of fluorinated pyrex and

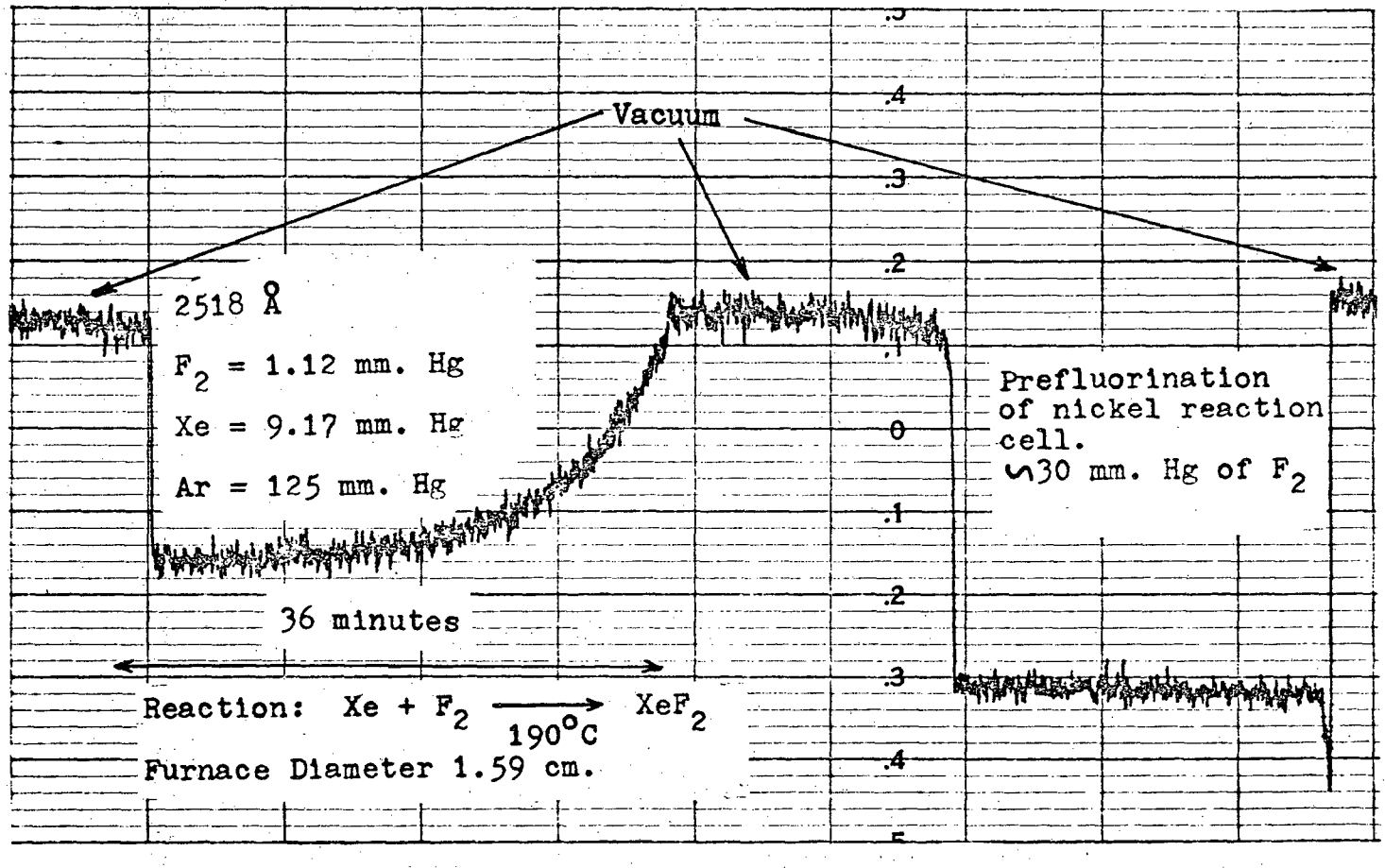

Figure 6. Typical Response Curve for the Reaction of Xenon and Fluorine in Excess Xenon

the Kel-F alkane[40], $Cl-(CF_2-CFCl)_5Cl$. The halogenated alkane was supplied by Minnesota Mining and Manufacturing Company. This manometer oil was quite inert to xenon and fluorine, but reacted readily with the xenon fluorides producing a yellow solution in the oil and a colorless gas. It has been previously reported[28] that xenon tetrafluoride reacts with Kel-F wax releasing chlorine. The manometer was connected to the stainless steel system by the following sequence: pyrex to copper seal, copper to brass weld, brass to stainless steel Viton o-ring seal. The oil density was reported[40] to be 1.93. The density of the sample used in this apparatus was determined to be 1.922. An advantage of this manometer liquid, in addition to inertness, was the seven fold increase in sensitivity over mercury. Disadvantages were the wetting of the pyrex by the oil and a vapor pressure of about fifty microns. It was found that some fresh samples of this material required several hours of outgasing under vacuum before use. The room temperature gas handling system was constructed of stainless steel, copper, and brass and thoroughly fluorinated. The exhaust system contained a sodium chloride in stainless steel reactor. Samples containing excess fluorine were pumped over the sodium chloride at 100°C. The fluorine was absorbed by reaction and the chlorine produced was removed by freezing in a pyrex trap at liquid nitrogen temperatures.

MATERIALS

The fluorine, xenon, and argon were obtained from Matheson Company. The fluorine was about 98 percent pure.[41] The major impurity was hydrogen fluoride[42] which was removed by passing the fluorine through a sodium fluoride trap also supplied by Matheson Company. The lack of etching in the dry pyrex manometer was an indication that the method was successful. The argon and xenon were used directly from the cylinders. The supplier claimed[41] that "Gold Label" argon contained less than 10 parts per million impurities and that "Research Grade" xenon contained approximately 50 parts per million impurities most of which was krypton. The xenon difluoride and xenon tetrafluoride were synthesized in the hot cell by using fluorine and xenon at appropriate pressures calculated from published equilibrium constants.[1]

SPECTRA

Fluorine

Fluorine has a broad continuous absorption produced by the allowed transition from the $^1\Sigma_g^+$ ground electronic state to the unbound excited $^1\Pi_u$ electronic state which dissociates to $^2P_{\frac{3}{2}}$ and $^2P_{\frac{1}{2}}$ (Figure 7) atomic fluorine.[21,43,44] The temperature dependence of the spectrum is produced by the changing populations of the vibrational energy states in the ground electronic state. The energy difference between the vibrational states is known to be 892 cm^{-1} from the Raman spectrum.[22,23] In the temperature region where the ground vibrational state and first excited vibrational state are the only ones significantly populated (see Table IV) the temperature dependence of the maximum can be calculated simply from ground state depletion. This provides a convenient check on the method since this number is also determined experimentally. It is listed in the literature for a 100°C range as -0.031%/deg.[14] determined in this work for a 227°C range to be -0.032%/deg. and calculated to be -0.031%/deg. In the range 250 to 400°C the second excited state is also of importance. The experimental results may be seen in Figure 8 and Table V.

It is stated in the literature that Beer's law was followed in the range 50 to 760 mm.[14] This work shows that Beer's law is also followed in the range 5 to 25 mm as may be seen in Figure 9 and Table VI.

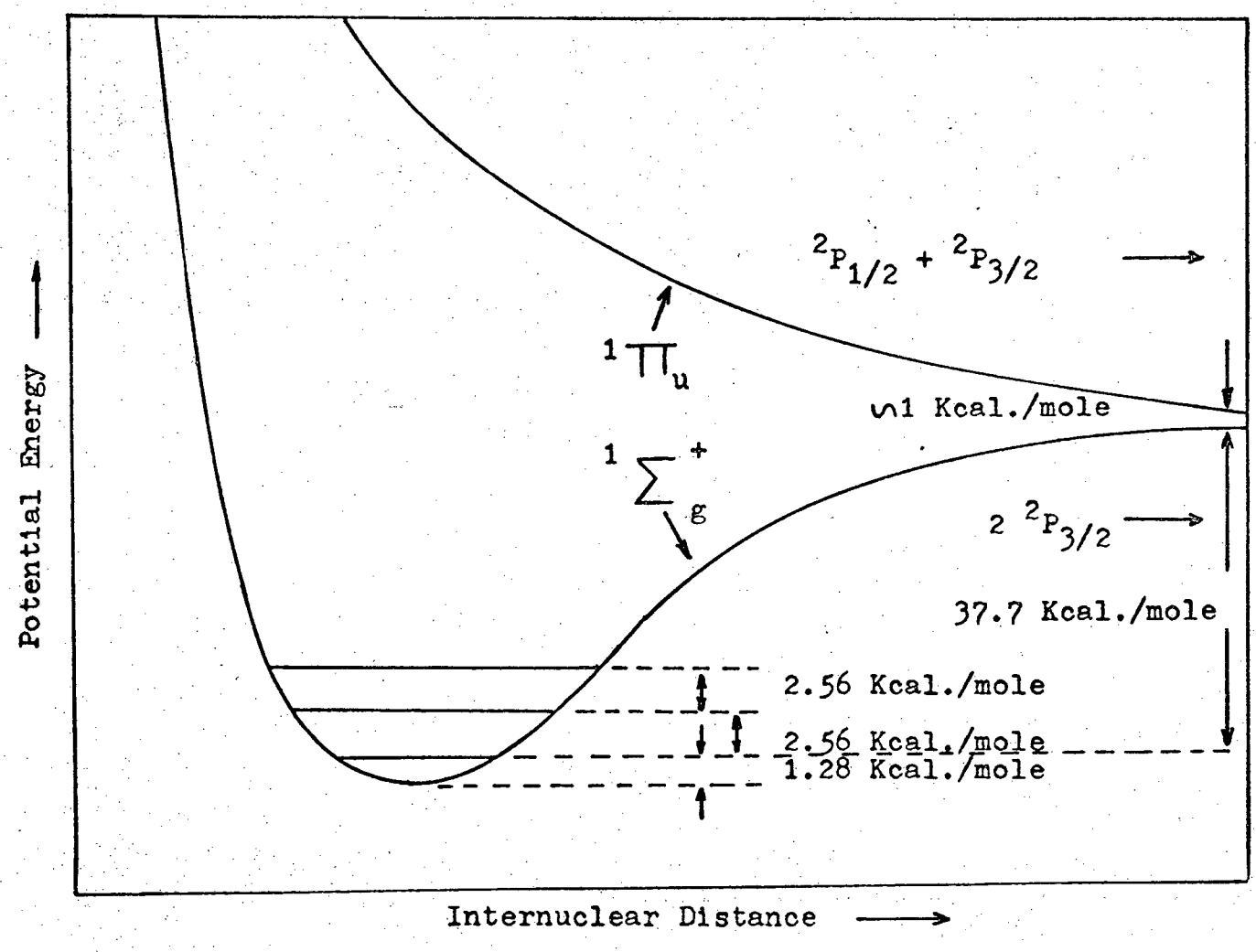

Figure 7. Potential Energy Diagram for Fluorine (not to scale).

Table IV

Thermal Excitation of Fluorine

Temperature (^{o}C)	Percent in State		
	Ground (n = 0)	First Excited (n = 1)	Second Excited (n = 2)
23	98.7	1.3	0.0
250	91.5	7.8	0.7
400	85.5	12.6	1.9

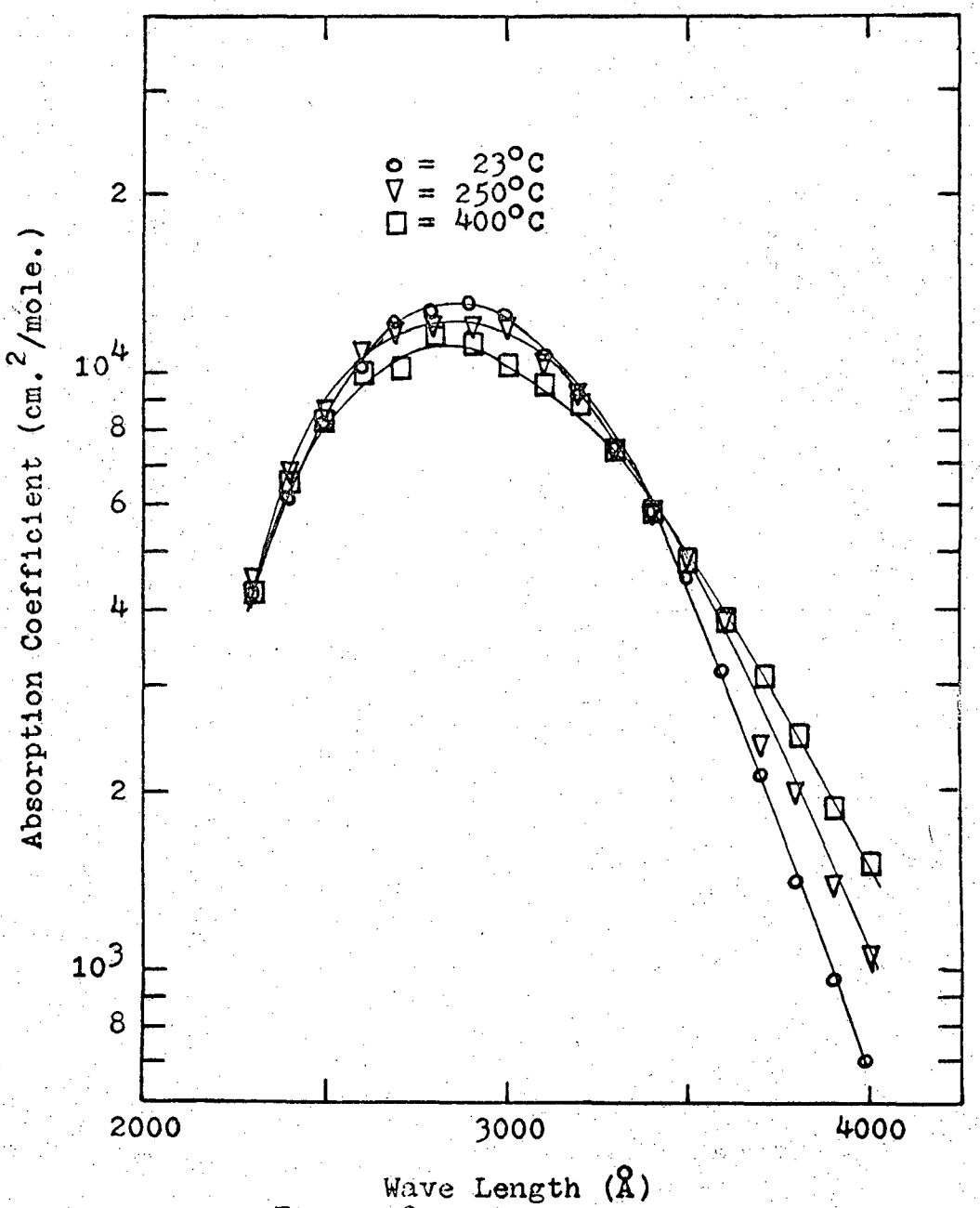

Figure 8. Fluorine Spectra

Table V

Absorption Coefficients* of Fluorine

Wave Length Å	Absorption Coefficients (cm^2/mole) x 10^{-4}		
	23°C	250°C	400°C
2318	0.442	0.466	0.418
2418	0.611	0.678	0.648
2518	0.822	0.855	0.802
2618	1.02	1.047	0.899
2718	1.20	1.189	0.996
2818	1.26	1.183	1.145
2918	1.32	1.190	1.113
3018	1.24	1.195	1.008
3118	1.08	1.052	0.938
3218	0.920	0.928	0.872
3318	0.751	0.761	0.713
3418	0.586	0.576	0.589
3518	0.451	0.496	0.478
3618	0.311	0.386	0.381
3718	0.209	0.236	0.312
3818	0.143	0.197	0.245
3918	0.0963	0.141	0.187
4018	0.0699	0.104	0.148

* See Footnote, p. 6.

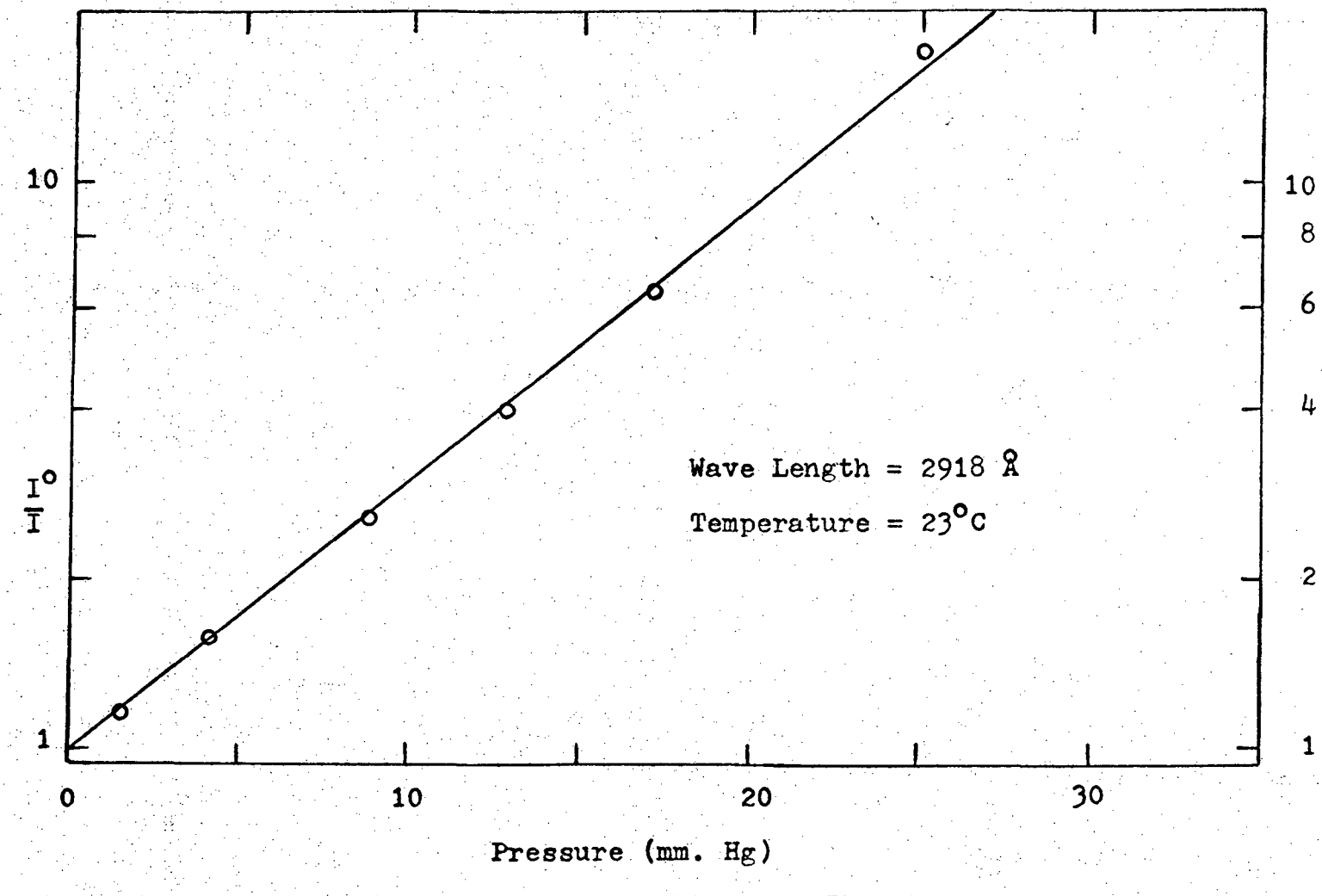

Figure 9. Beer's Law Plot for Fluorine

Table VI

Beer's Law Data for Fluorine at 2918 Å

I^o/I	Pressure of Fluorine (mm Hg)
17.0	25.2
6.40	17.3
3.92	12.8
2.55	8.9
1.54	4.3
1.34	3.0
1.16	1.7

Xenon Difluoride

The ultraviolet spectrum of xenon difluoride at room temperature has been reported in the literature.[15-17] In the near ultraviolet region there is a broad absorption band (Figure 10) which peaks at 2330 Å. This has been assigned to a symmetry forbidden transition which borrows intensity from the 1580 Å band by vibronic coupling involving the Π_u vibrations of the linear xenon difluoride. Since the Π_u frequency of xenon difluoride is low (213 cm^{-1}) a relatively high temperature dependence is expected. From the literature experimental information up to 120°C. yields an increase of 0.12 $\pm$ .04%/deg. Theory predicts 0.3%/deg. Thus a large increase in intensity is observed but less than predicted. This is the common experimental result[45-48] and is expected to continue at higher temperature.

At more elevated temperatures dissociation ($XeF_2 \rightleftharpoons Xe + F_2$) and reaction ($2XeF_2 \rightleftharpoons Xe + XeF_4$) of xenon difluoride may occur. Thus a ten to one mixture of xenon and xenon difluoride respectively was used to measure the absorption spectrum since both of these reactions can be inhibited by excess xenon which is transparent in the near ultraviolet region. The results may be seen in Figure 10 and Table VII. The temperature dependence was 0.11%/deg.

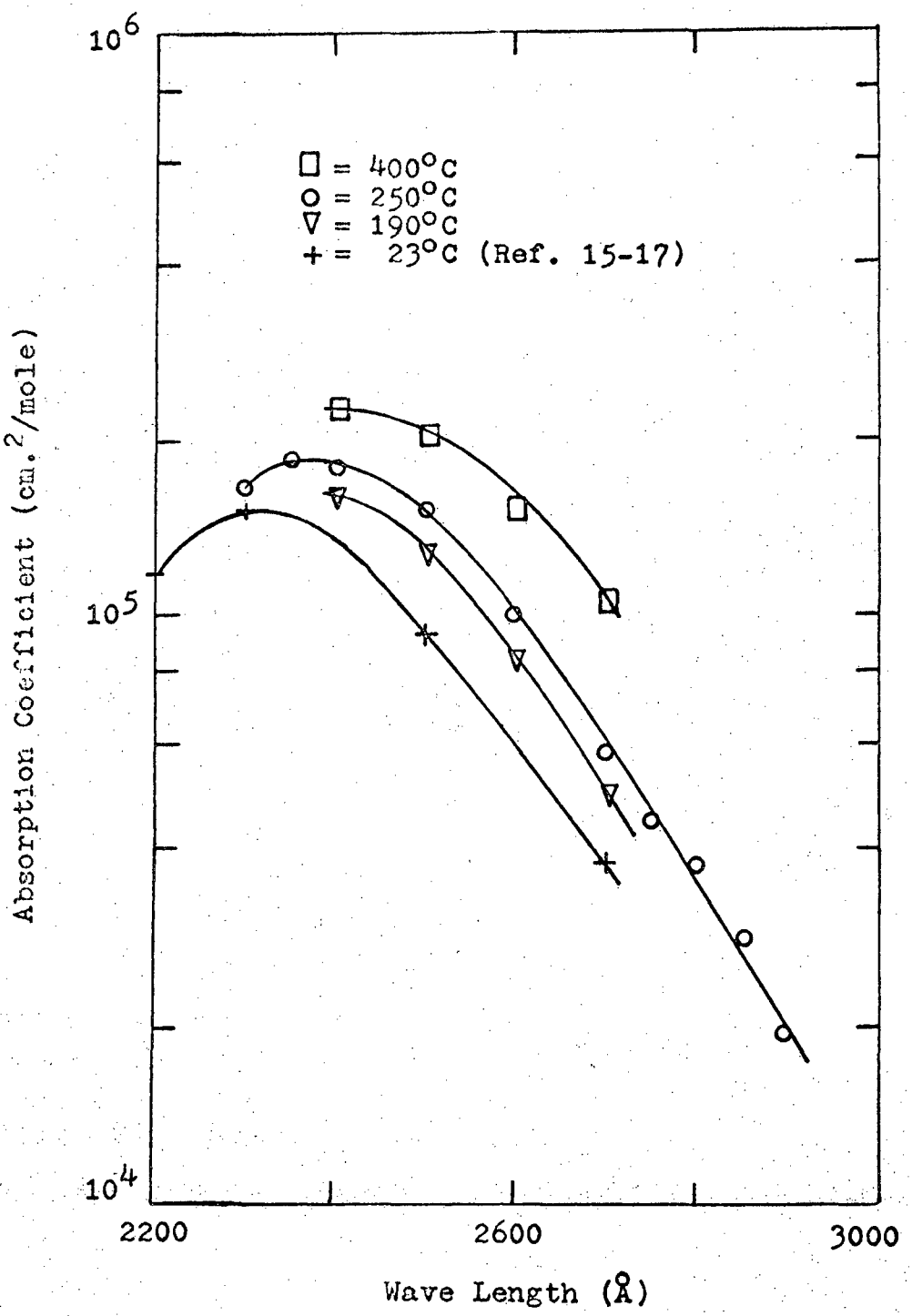

Figure 10. Xenon Difluoride Spectra

Table VII

Absorption Coefficients* of Xenon Difluoride

Wave Length Å	Absorption Coefficients (cm^2/mole) x 10^{-5}		
	190°C	250°C	400°C
2318		1.65	
2368		1.85	
2418	1.60	1.78	2.43
2518	1.26	1.50	2.09
2618	0.83	0.990	1.55
2718	0.49	0.580	1.05
2768		0.450	
2818		0.370	
2868		0.278	
2918		0.195	

* See Footnote, p. 6.

Xenon Tetrafluoride

The ultraviolet spectrum of xenon tetrafluoride at room temperature has been reported in the literature.[15,16,18] In the near ultraviolet region there is a broad absorption band which peaks at 2280 Å (Figure 11) which has been assigned to a spin forbidden transition which borrows intensity from the 1580 Å band by spin orbit coupling. In addition there is a shoulder on the above broad band near 2580 Å which was assigned to a symmetry forbidden transition which borrows intensity from the 1325 Å band by vibronic coupling involving the 221 cm^{-1} b_{1u} and the 291 cm^{-1} a_{2u} vibrations of the square planar xenon tetrafluoride. Consequently this shoulder is expected to show a greater temperature dependence than the 2280 Å peak.

At elevated temperatures dissociation ($XeF_4 \rightleftharpoons XeF_2+F_2$) can occur.[1] To inhibit this reaction a ten to one mixture of fluorine and xenon tetrafluoride respectively was used while measuring the absorption spectrum. Fluorine itself absorbs in this region but does not seriously interfere because the absorption coefficients of the xenon tetrafluoride ranges from ten to one hundred times that of fluorine. The experimental results may be seen in Figure 11 and Table VIII.

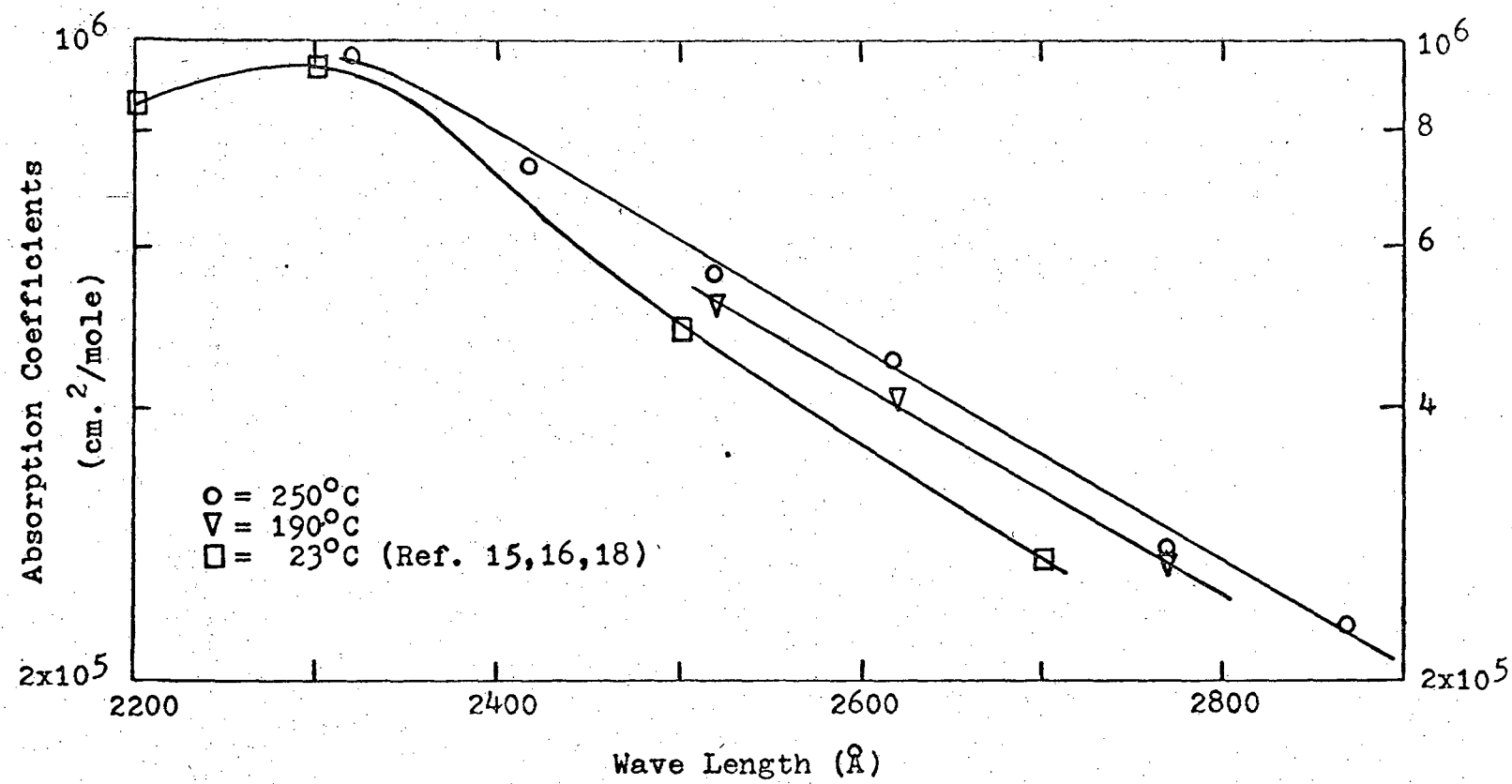

Figure 11. Xenon Tetrafluoride Spectra

Table VIII

Absorption Coefficients* of Xenon Tetrafluoride

Wave Length Å	Absorption Coefficients $(cm^2/mole) \times 10^{-6}$	
	190°C	250°C
2318		0.95
2418		0.74
2518	0.53	0.55
2618	0.42	0.45
2768	0.27	0.28
2868		0.23

* See Footnote, p. 6.

Fluorine: Theoretical Analysis

The continuous absorption of chlorine[49,50] has been treated theoretically in detail.[49,51,52] These papers provide a model for a similar analysis which is in progress[53] for the fluorine spectra. The method consists of an approximation of the unbound electronic state potential function and the electric moment of fluorine from measured absorption coefficients at room temperature. This information can be used to calculate partial absorption coefficients for individual excited vibrational states and hence the total absorption coefficients of fluorine at elevated temperatures.

KINETICS PROCEDURE

Mechanical Operation

The procedure used for the kinetic experiments first involved adjusting the temperature distribution by varying the voltage applied to the various heating elements until a uniform temperature distribution was obtained. For temperatures up to 250°C window cooling was unnecessary. The Viton o-rings were stable in air or vacuum to 250°C. They were also stable at this temperature for extended periods with low pressure fluorine (<1/20 atm.), but finally became flattened, lost their resilience, and partially deteriorated forming a graphite-like powder. At more elevated temperatures the window region was water cooled. This produced a 6.35 cm region on each end of the reaction cell which was at lower temperatures than the central remaining 133.3 cm, thus requiring end corrections which will be discussed later. After thermal steady state had been reached the system was fluorinated until no further decrease in pressure was noticed on the manometer. The gases were mixed at the desired pressure in a 1,750 cc stainless steel tank. Immediately before expanding the gas mixture into the reaction cell, the cell was again fluorinated as may be seen in Figures 6 and 12. This procedure was essential to obtain reproducible data. Even so, the first run of a series frequently had to be discarded because of obvious reactor

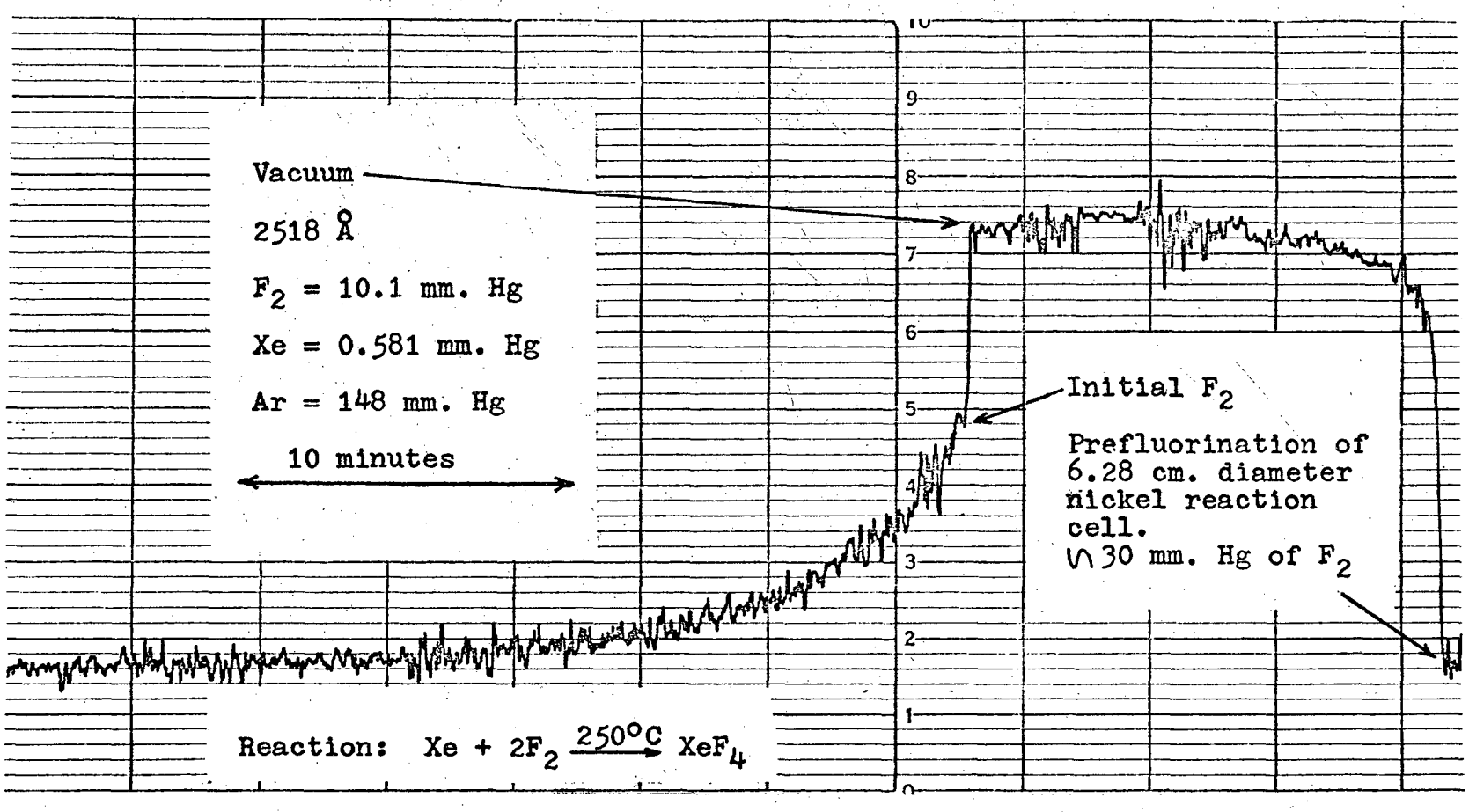

Figure 12. Typical Pair of Response Curves for the Reaction of Xenon and Fluorine in Excess Fluorine

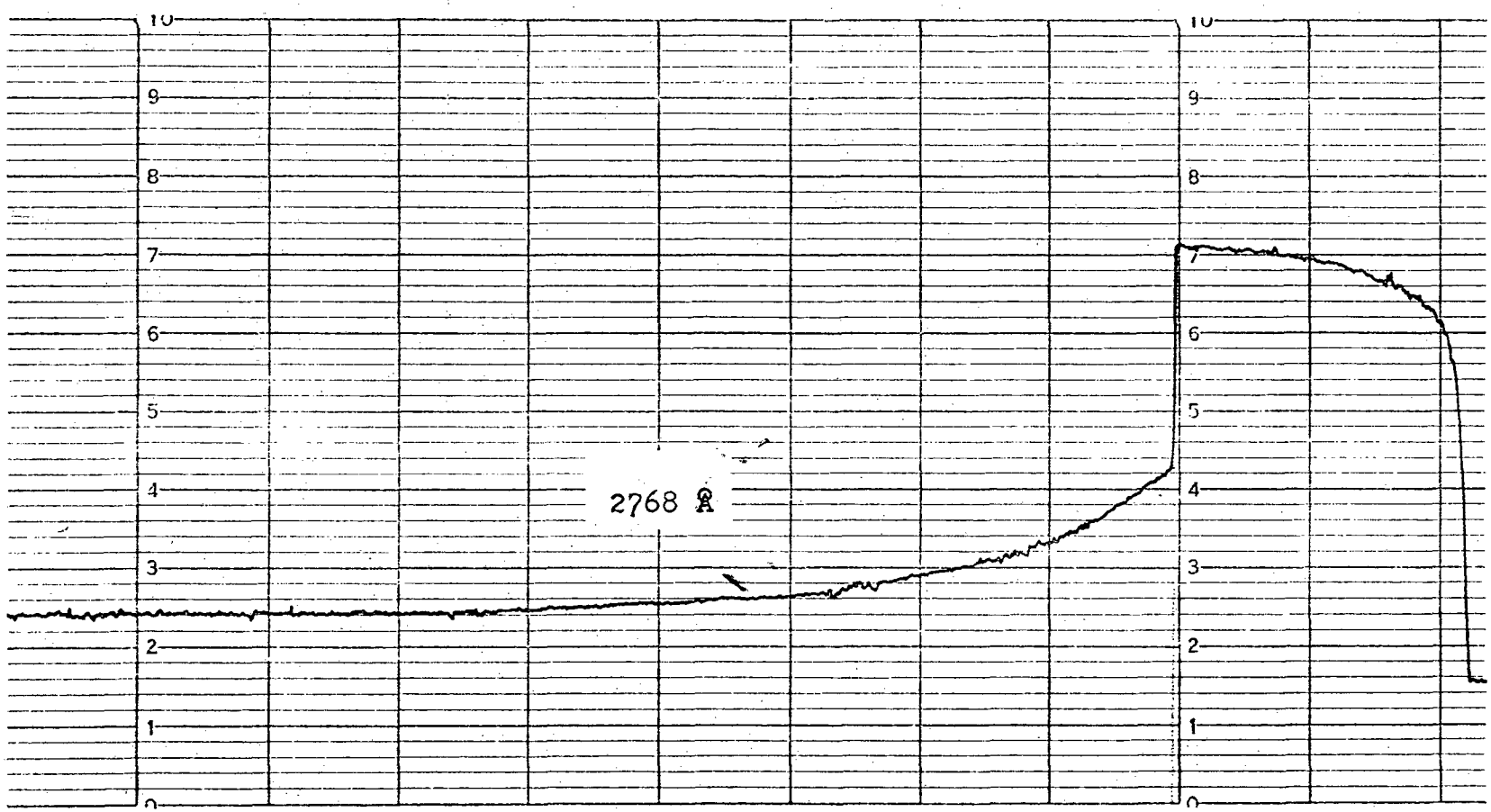

Figure 12. (Continued) Typical Pair of Response Curves for the Reaction of Xenon and Fluorine in Excess Fluorine

fluorination. After the cell was properly seasoned as described the gas mixture was expanded into the hot cell. The gas flow required from one to two seconds after which the valves on both sides of the cell were immediately closed and the pressure was read on either the oil manometer or the Monel Helicoid gage. Pressure readings were avoided during the reaction period to prevent the exposure of the hot gases to cold surfaces. The transmission was automatically recorded during the run which was continued until no further change was observed.

Absence of Xenon Hexafluoride

Of the three compounds xenon difluoride, xenon tetrafluoride, and xenon hexafluoride previously mentioned it is believed that the xenon hexafluoride did not form during these experiments even though the equilibrium constants would suggest it might. One reason is that even under the tens to hundreds of atmospheres used in its synthesis sixteen hours[6] to ten days[32] of reaction time were required. A second reason for doubting the presence of xenon hexafluoride is that the xenon hexafluoride absorbs strongly[1,19] below 2750 Å while both xenon difluoride[15-17] and xenon tetrafluoride[15,16,18] are weak absorbers. Consequently significant amounts of xenon hexafluoride would have caused the system to become opaque in the 2500 Å region where most of the experiments

were made. A third somewhat weaker reason is that the conditions under which pure xenon tetrafluoride is synthesized[1,4-6] indicate that a large fraction of xenon hexafluoride should have formed if equilibrium had been obtained. The pressures used in the xenon tetrafluoride syntheses were much higher than those used in the experiments in this report and the time period was about the same. Further evidence indicating the absence of xenon hexafluoride will be presented later.

General Equations

In the absence of xenon hexafluoride the following equations apply. The symbols used below and throughout the rest of this report are defined in Table IX. Conservation of mass yields:

$$C_1 + C_2 + 2C_4 = C_1^o$$

$$C_o + C_2 + C_4 = C_o^o$$

and the optical absorption gives:

$$a_1C_1 + a_2C_2 + a_4C_4 = (1/L)\ln(I^o/I)$$

$$a_1'C_1 + a_2'C_2 + a_4'C_4 = (1/L)\ln(I^o/I)'$$

The prime indicates a second wave length. Wave lengths suitable for these experiments are those for which all of the species, excepting xenon, absorb strongly. It is also desirable for sensitivity that the slope of the

Table IX

Definition of Symbols

a = Absorption Coefficient (cm^2/mole)
(See Footnote p. 6)

C = Concentration (moles/cc)

I = Intensity

L = Length (cm)

P = Pressure (atm.)

<u>Subscripts</u>:

o = Xenon

1 = Fluorine

2 = Xenon Difluoride

4 = Xenon Tetrafluoride

<u>Superscripts</u>:

o = Initial

∞ = Final or equilibrium

n = Algebraic exponent

absorption coefficient versus wave length function of one differs in sign from that of the other two. From Figure 3 it can be seen that 2500 Å and 2750 Å fit these requirements. Figure 5 curve A indicates that the apparatus is also sensitive in this region. Hence these wave lengths (2518 Å and 2768 Å after calibration) were those most frequently used.

Discussion of Problems

Since the ultraviolet light is being used to follow thermal reactions one must be certain that photochemical reactions are not occurring. Bausch & Lomb data sheets indicate that the combination of the Deuterium Lamp and single monochromator produce a maximum of 32 microwatts at a slit width of 3 mm. The second monochromator, the smaller slit width used, the Quartz Fluorite Condenser, and the calcium fluoride window will strongly reduce this number. Thus the rate at which photons enter the reaction cell can be shown to be less than 5×10^9 photons per second. This is six orders of magnitude less than Weeks and Matheson used[40] in photochemical studies of xenon-fluorine reactions. Thus no detectable photolysis is expected under these experimental conditions. To further confirm this conclusion samples similar to those used at elevated temperatures were exposed to the ultraviolet light at room temperature for several hours. No reaction was detected.

Optical effects from reactions of impurities in the reagents from reactions of air from undetected leaks with the reagents, or from reaction with the tanks was checked experimentally. It was found that the following materials or mixtures at room temperature, 250°C and 400°C gave no indication of reaction:

1. Fresh fluorine.
2. Fluorine stored several days in a stainless steel tank.
3. Fluorine mixed with undried air.

This sequence was repeated for xenon, argon, fluorine and argon, and xenon and argon. These experiments did not eliminate the possibility of an impurity from fluorine reacting with an impurity from xenon. However, the purity level of "Research Grade" xenon makes this possibility remote.

Optical effects from the vapor of the manometer oil were also considered. The transmission of the cell was checked from 2318 to 4018 Å with the manometer in and out of the system. No optical effect was noticed at any wave length. The manometer was down stream from the reaction cell (see Figure 4) which avoided pumping the Kel-F vapor through the hot region. The cell was always flushed before an experiment by the fluorination procedure and was cut off from the manometer during reaction.

Expanding the gas mixture into the cell was accompanied by several temperature effects. First there was cooling of the gas in the mixing tank which further reduced

its pressure. This, however, did not change the ratio of the gases present. Hence, the measurement of the pressure after the gas was added to the cell avoided errors, due to cooling, in the determination of initial concentrations. The use, for instance, of volume ratios was quite unsatisfactory here. This cooling was immediately followed by rapid heating in the reaction cell. Since the relative heat capacity of the gas and cell wall was in the range of 10^5 or 10^6 cooling of the cell by the gas was of no significance. Heating of the gas by the cell in the case of fluorine spectral measurements at pressures as high as 10^{-1} atmospheres was faster than the response time of the apparatus which varied between 0.3 and 1.0 second. The lower value was the response time of the recorder while the high value was produced by filters in the amplifier.

Aside from heat effects of sample manipulation the reaction itself can alter the temperature of the system.[54,55] It can be shown from relations given in these references that internal heating of the gas by homogeneous reaction is $<1^{\circ}C$. On the other hand for a heterogeneous reaction the large heat sink provided by the nickel pipe should avoid large temperature effects since <5 calories were released in a several minute period.

Expansion of the nickel cell was 6 mm from room temperature to $400^{\circ}C$. This was less than 0.5 percent of

the length and was neglected.

Water cooling of the window produced effects some of which were important. Since gas molecules may diffuse between the window and the hot region in a matter of one or two minutes and convection will also occur complete mixing is assumed. However, the pressure of the xenon difluoride or xenon tetrafluoride could not be allowed to exceed its vapor pressure at room temperature (see Figure 2). Also gases concentrated in the cooler ends and absorbed radiation more strongly per unit path length than the hot gases. This was by far the largest end effect and required a correction of as much as 11% to be made on some of the experimental values of $\ln(I^{o}/I)$ at the highest temperatures.

Since the maximum temperature effect on the absorption coefficients was about 20% and the cooled end regions made up about 9% of the path length the maximum value of this end effect was about 2%. This was neglected. The residence time of the reactants in the hot cell was reduced by about 1%. This also was neglected. For temperatures of 250°C or less the windows were uncooled, and end effects were not important.

THE REACTION OF XENON AND FLUORINE IN EXCESS XENON

The Reaction $Xe + F_2 \longrightarrow XeF_2$: General Considerations

The equilibrium constants in Table I and Figures 1a and 1b were used to calculate concentrations of xenon and fluorine which will lead to the formation of sufficient xenon difluoride to be followed easily by optical means, but with too little xenon tetrafluoride to be seen. Typical starting values for this condition are about one mm of fluorine and ten or more mm of xenon. The reaction goes to completion within limits of detection.

Under these conditions the equations on page 39 simplify to:

$$C_1 + C_2 = C_1^o$$

$$C_o + C_2 = C_o^o$$

$$a_1C_1 + a_2C_2 = (1/L)\ln(I^o/I)$$

Only one wave length was necessary here and it was usually 2518 Å. The equations lead to:

$$a_2 = (1/C_2^{oo}L)\ln(I^o/I)^{oo} = (1/C_1^oL)\ln(I^o/I)^{oo}$$

which allows a determination of a_2 for each experiment and to:

$$C_2 = (L^{-1}\ln(I^o/I) - a_1C_1^o)(a_2-a_1)^{-1}$$

$C_1 = C_1^o - C_2$

$C_o = C_o^o - C_2$

The XeF free radical which is known to exist and which may absorb near 2500 Å could interfere with these calculations if its concentration were high enough. Reference 29 indicates that its concentration is about three orders of magnitude lower than that of xenon difluoride at temperatures near 400°C. However, since absorption coefficients for XeF are unknown and could be more than three orders of magnitude higher than those of xenon difluoride optical effects of XeF might be important. Duplicate experiments at different wave lengths were made to determine its effect. One such comparison at 250°C may be seen in Table IXa. Experiments 16 and 17 are duplicates except that the wave length was changed from 2518 to 2618 Å. A similar set of experiments were conducted at 400°C. No effect indicating XeF interference was found.

A typical response curve may be seen in Figure 6. A typical set of concentrations versus time are shown in Figure 13 and Appendix Table IA.

Variable Dependence

The dependence of the reaction rate on an inert gas was checked with argon. One set of results at 190°C are shown in Table IXa, experiments 1-4. No effect was

Table IXa

Rate Constants

Experiment Number	Temperature (°C)	Furnace Diameter (cm)	Initial Pressures (mm Hg) F_2	Xe	Ar	Constants (sec^{-1}) x 10^3 k_2	k_2'	k_4
1[a]	190	1.59	1.04	9.21	0	2.8		
2	190	1.59	1.12	9.17	125	2.9		
3	190	1.59	1.00	9.19	295	3.3		
4	190	1.59	1.06	9.16	406	3.0		
5	190	1.59	1.03	20.1	125	2.9		
6	190	1.59	1.07	29.9	127	3.2		
7	190	1.59	1.05	40.2	124	2.9		
8[b]	250	6.28	10.2	0.593	0		10.2	3.0
9	250	6.28	10.1	0.581	148		9.7	3.2
10	250	6.28	10.0	0.590	300		10.4	3.0
11	250	6.28	9.9	0.579	398		9.8	3.2
12	250	6.28	13.1	0.591	149		10.1	3.3
13	250	6.28	15.9	0.584	148		9.6	3.4
14	250	6.28	19.8	0.573	151		10.3	3.1

Table IXa (Contd.)

Rate Constants

Experiment Number	Temperature (°C)	Furnace Diameter (cm)	Initial Pressures (mm Hg)			Constants (sec^{-1}) x 10^3		
			F_2	Xe	Ar	k_2	k_2'	k_4
15[c]	250	6.28	10.2	0.585	150		10.1	3.3
16	250	6.28	1.08	13.0	15	2.2		
17[d]	250	6.28	1.05	13.2	16	2.1		

[a] Wave Length for 1-7 and 16 was 2518 Å.
[b] Wave Lengths for 8-14 were 2518 and 2768 Å.
[c] Wave Lengths increased to 2618 and 2868 Å.
[d] Wave Length increased to 2618 Å.

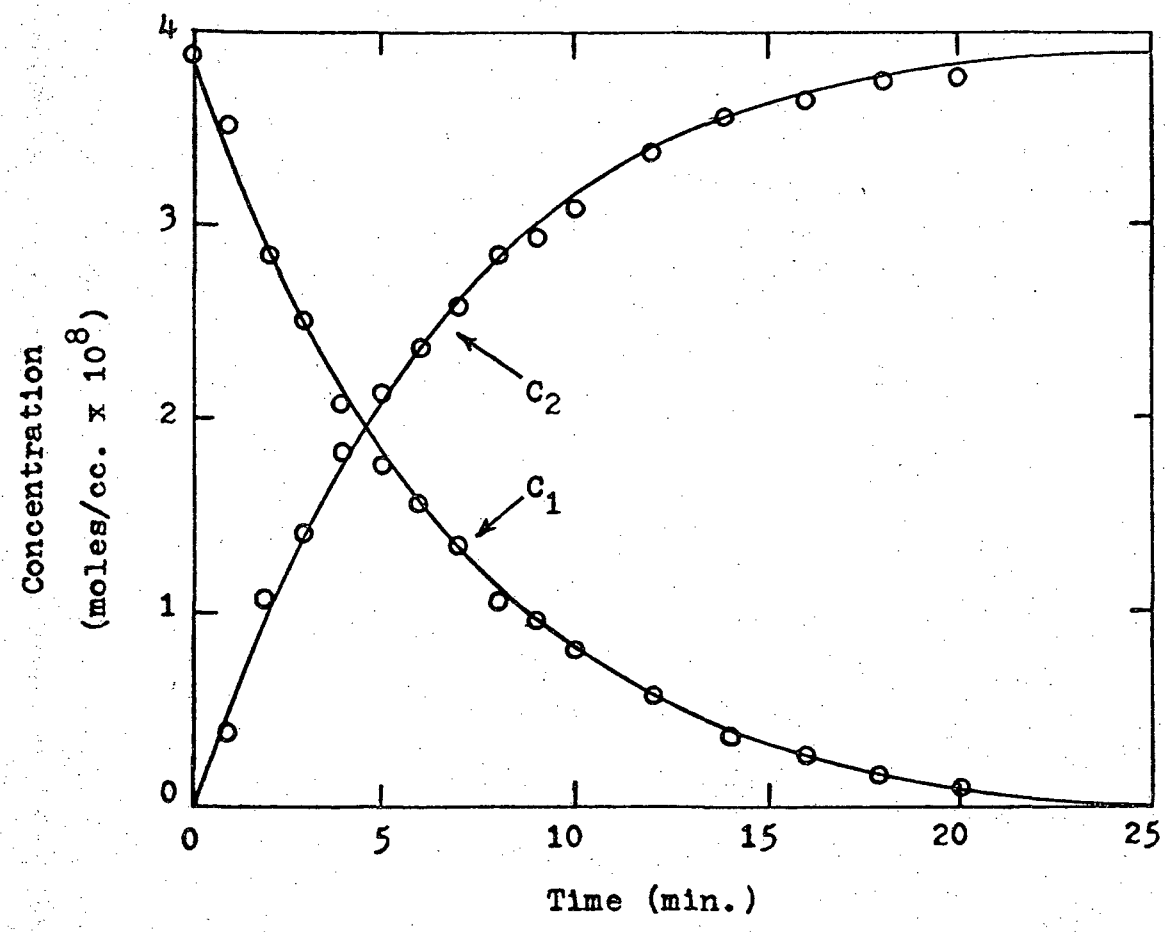

Figure 13. Typical Set of Concentration Curves for the Reaction of Xenon and Fluorine in Excess Xenon

noticeable. Similar experiments were also made at 250°C and 400°C to further confirm this behavior. Hence argon was used in subsequent experiments to provide a higher pressure which aided gas flow by providing higher pressure differentials.

The reaction rate was first order in fluorine. This behavior may be seen for a typical case in Figure 14 and Appendix Table IA.

The reaction rate was zero order with respect to xenon as demonstrated by experiments 2,5-7 at 190°C in Table IXa. Similar experiments were also made at 250°C and 400°C to confirm this behavior. The constants from experiments 1-7 were averaged and entered in Table X under the 190°C, small furnace heading. Thus the rate expression under these conditions was $dC_2/dt = k_2C_1$.

The geometric surface to volume ratio differed by a factor of four between the two furnaces. The reaction rate was lower by a factor of thirteen at 250°C in the larger furnace. Hence the reaction was heterogeneous.

An Arrhenius plot for these reaction rate constants at various temperatures is shown in Figure 15. The activation energies and the pre-exponential factors are shown in Table XI.

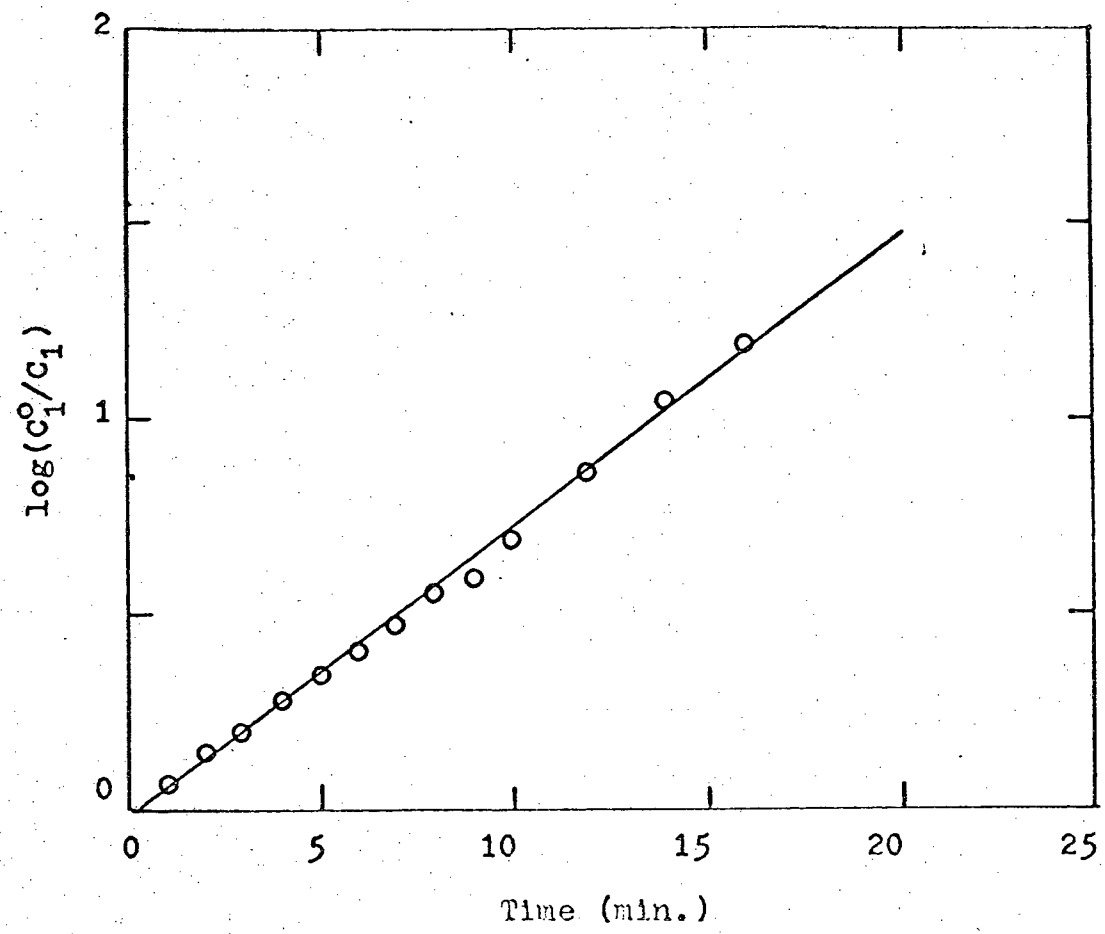

Figure 14. Typical Fluorine Behavior for the Reaction of Xenon and Fluorine in Excess Xenon

DELETED

Table X

Rate Constants

Temperature (°C)	Constants (sec.$^{-1}$) x 10^3					
	k_2		k_2'		k_4	
	SF[a]	LF[b]	SF	LF	SF	LF
190	3.0		30	2.0	10	0.68
225	9.8		∿72	6.2	25	1.8
250	23	1.8	∿150	10	∿50	3.2
290		4.3				
330		12				
400		38				

[a] SF = Small Furnace, 1.59 cm diameter.
[b] LF = Large Furnace, 6.28 cm diameter.

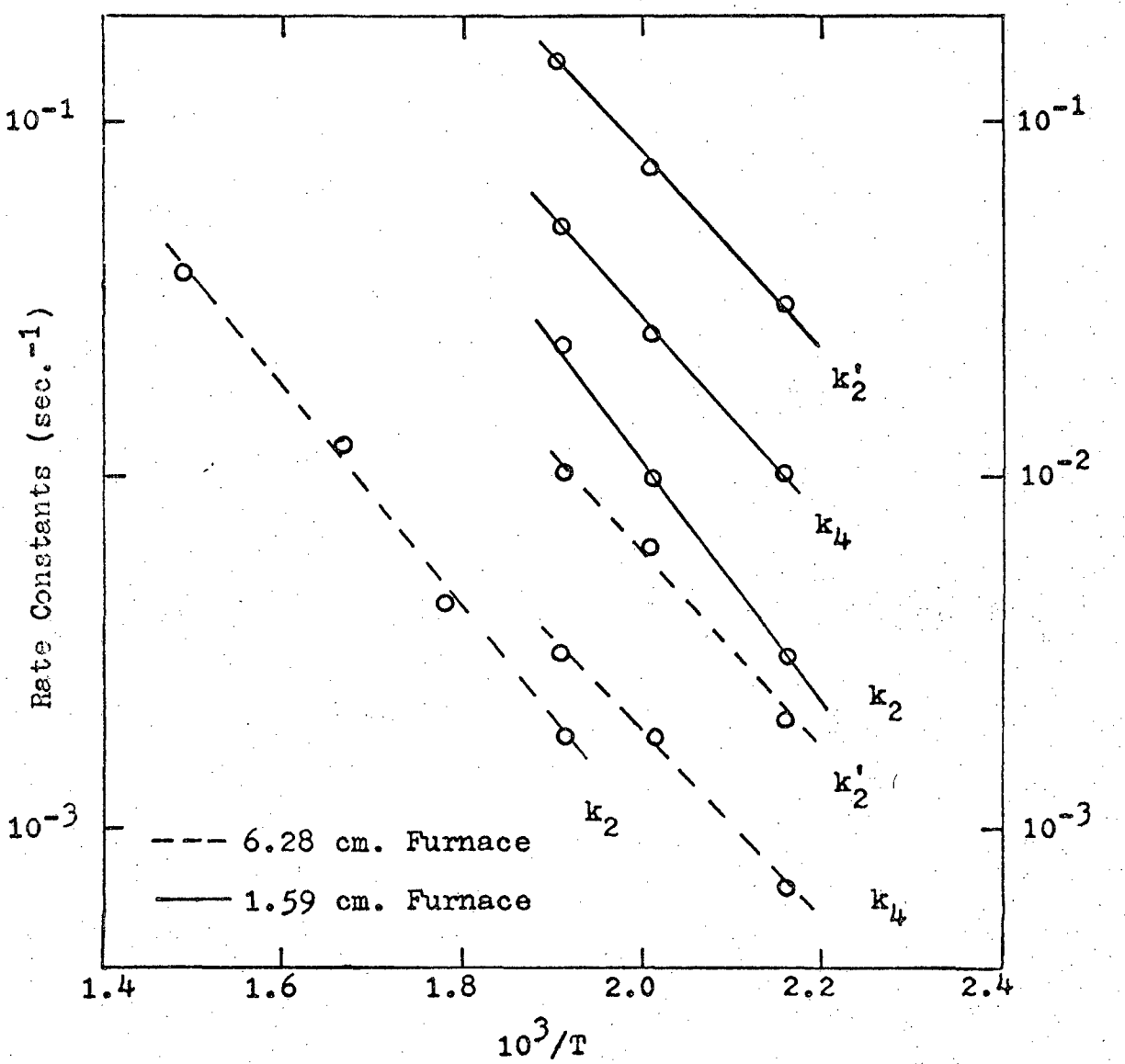

Figure 15. Arrhenius Plots for the Rate Constants

Table XI

Activation Energies and

Pre-exponential Factors

Activation Energy	Pre-exponential Factor		Associated with:
(kcal./mole)	(sec.$^{-1}$) x 10^{-4}		
14.3	00.22	k_2	LF[a]
15.7	14.		SF[b]
12.4	0.23	k_2'	LF
13.2	7.7		SF
12.8	0.048	k_4	LF
13.	2.1		SF

[a] LF = Large Furnace, 6.28 cm diameter.
[b] SF = Small Furnace, 1.59 cm diameter.

THE REACTION OF XENON WITH FLUORINE IN EXCESS FLUORINE

The Reaction $Xe + 2F_2 \longrightarrow XeF_4$: General Considerations

The equilibrium constants in Table I and Figures 1a and 1b along with the assumption that xenon hexafluoride is absent, may be used to calculate concentrations of xenon and fluorine which will lead to the formation of xenon tetrafluoride with an insignificant final amount of xenon difluoride. Initial pressures of 0.6 mm. of xenon and ten or more mm. of fluorine satisfied this requirement and also provided concentrations of fluorine, xenon difluoride and xenon tetrafluoride which could be followed optically. The optical requirement was twofold. None of the three materials , fluorine, xenon difluoride, or xenon tetrafluoride, must be present in too small a concentration to be detected for any extended time nor may any one be present in such a high concentration that the system be opaque.

Under these conditions the full set of equations on page 39 must be used. They lead to the following solutions:

$$a_4 = \left[(1/L)\ln(I^o/I)^\infty - a_1C_1^\infty - a_2C_2^\infty\right](1/C_4^\infty) =$$

$$= \left[(1/L)\ln(I^o/I)^\infty - a_1C_1^\infty\right](1/C_4^\infty)$$ since the experiment

is designed to produce little xenon difluoride in the final mixture. This allows a determination of a_4 and a_4' for each experiment.

Further:

$$C_4 = \left[(a_1-a_2)/A\right]\left[(a_1'/L)\ln(I^o/I) - (a_1/L)\ln(I^o/I)'\right]$$

$$- (B/A)\left[a_1C_1^o - (1/L)\ln(I^o/I)\right]$$

$$C_2 = \left[1/(a_1-a_2)\right]\left[a_1C_1^o - (1/L)\ln(I^o/I) - (2a_1-a_4)C_4\right]$$

$$C_o = C_o^o-C_2-C_4$$

$$C_1 = C_1^o-C_2-2C_4$$

where:

$$B = (a_1'a_2-a_1a_2') \text{ and}$$

$$A = (a_1-a_2)(a_1'a_4-a_1a_4') - (2a_1-a_4)B$$

As with the reaction terminating with xenon difluoride the possibility of other species being present must be considered. In this case xenon hexafluoride was of particular concern being favored by the excess fluorine. Duplicate experiments were made with two different pairs of wave lengths to investigate this possibility. The wave length pairs were 2518, 2768 and 2618, 2868 Å.

No effect was found as may be seen by comparing, in Table IXa, experiments 9 and 15 which differ only in the wave length used. This is a further confirmation of the absence of xenon hexafluoride formation previously discussed (pp. 38 and 39) under these experimental conditions.

A typical set of response curves may be seen in Figure 12. A typical set of concentrations versus time is shown in Figure 16 and Table XXVIIA of the Appendix.

Variable Dependence for $Xe + F_2 \longrightarrow XeF_2$

The dependence of the reaction rate on an inert gas was checked with argon. Experiments 8-11 at 250°C in Table IXa show no effect. This behavior was further confirmed by another set of similar experiments at 190°C.

The reaction rate was first order in xenon. The behavior may be seen for a typical case in Figure 17 and Appendix Table XXVIIA.

Experiments 9, 12-14 at 250°C in Table IXa indicate no effect from increased pressures of fluorine. This behavior was observed again at 190°C by another set of similar experiments. Thus the rate expression was $dC_o/dt = -k_2'C_o$ for the initial reaction producing xenon difluoride. The constants from experiments 8-15 were averaged and entered into Table X under the 250°C, large furnace heading.

The geometric surface to volume ratio was varied, as in the xenon difluoride terminating case, by a factor of

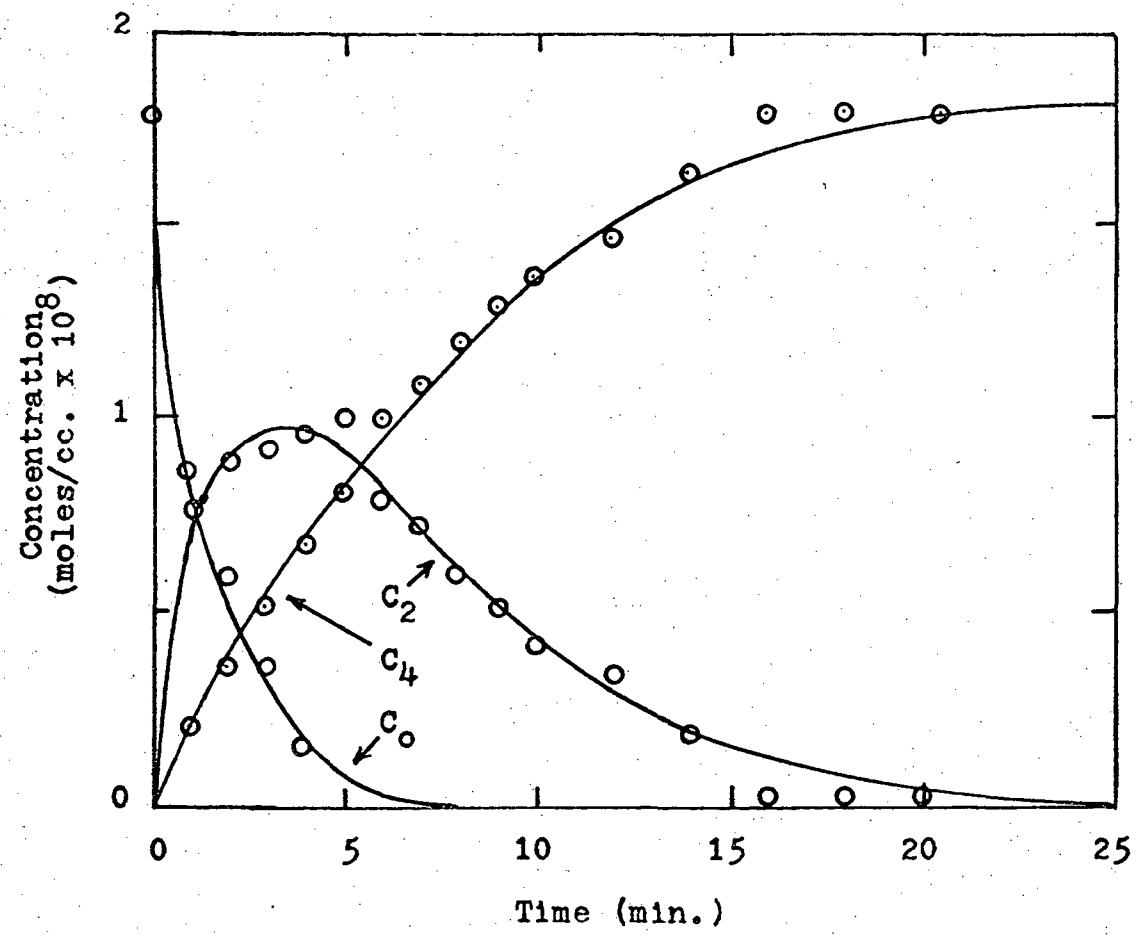

Figure 16. Typical Set of Concentration Curves for the Reaction of Xenon and Fluorine in Excess Fluorine

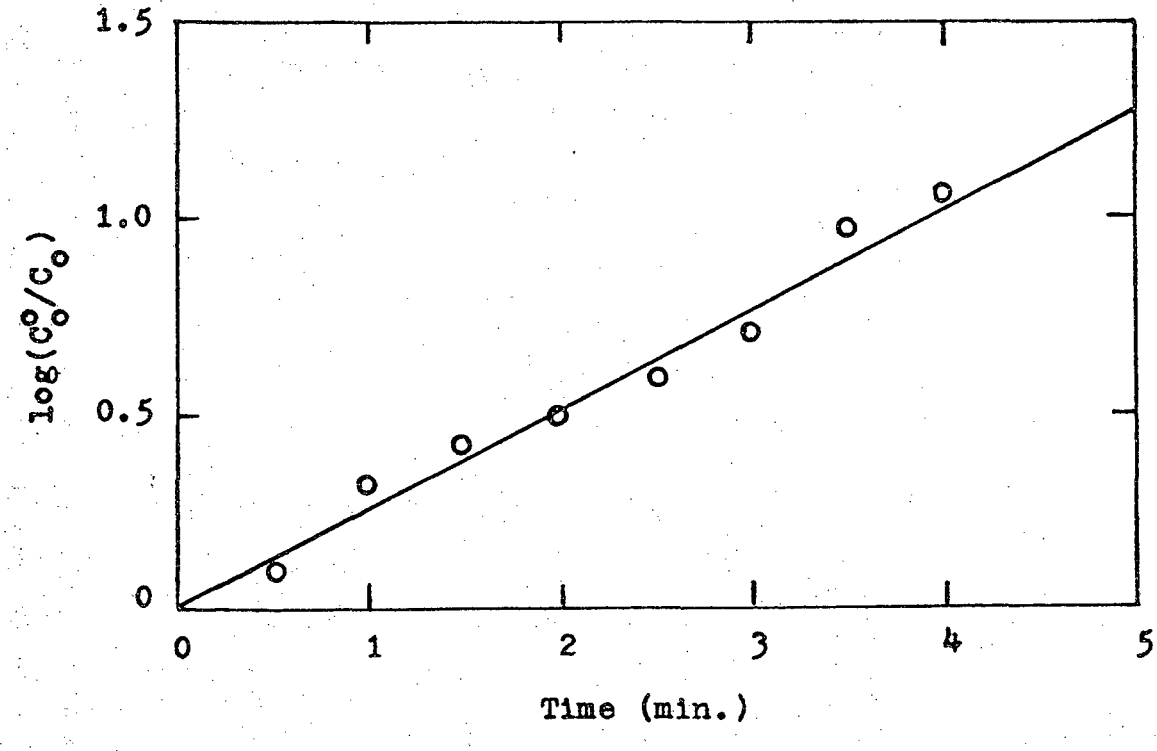

Figure 17. Typical Xenon Behavior for the Reaction of Xenon and Fluorine in Excess Fluorine

four. The reaction rates were slower by a factor of fifteen in the larger furnace. Hence the reaction was heterogeneous.

An Arrhenius plot for these reaction rate constants at various temperatures is shown in Figure 15. The activation energies and the pre-exponential factors are shown in Table XI.

<u>The Reaction $XeF_2 + F_2 \longrightarrow XeF_4$</u>

The rate of reaction of xenon difluoride and fluorine may be calculated from the previous data for the formation of xenon tetrafluoride from xenon and fluorine. This was done by assuming the following rate expression:

$$dC_4/dt = k_4 C_2^n$$

Thus

$$C_4(t) = k_4 \int_0^t C_2^n(t)dt = k_4 g^n(t)$$

and

$$C_4(t)/g^n(t) = k_4$$

The $g^n(t)$'s were obtained by graphical integration of $C_2(t)$ on plots like Figure 16. In Table XII based on Figure 16 and Appendix Table XXVIIA it may be seen that k_4 is constant if n=1 indicating that $dC_4/dt = k_4 C_2$. Argon and fluorine concentrations had no effect on the

Table XII

The Rate Constant k_4

Time (min.)	$C_4(t)$ (moles/cc) x 10^8	$g(t)$ (mole min./cc) x 10^8	$C_4(t)/g(t)$ (min.$^{-1}$) (k_4)	(sec.$^{-1}$) (k_4 x 10^3)
0	0.00	0.00		
1	0.16	0.56	0.29	4.8
2	0.36	1.36	0.26	4.3
3	0.51	2.26	0.23	3.8
4	0.67	3.21	0.21	3.5
5	0.81	4.16	0.19	3.2
6	1.00	5.06	0.20	3.3
7	1.09	5.81	0.19	3.2
8	1.20	6.46	0.19	3.2
9	1.30	7.01	0.19	3.2
10	1.36	7.44	0.18	3.0
12	1.47	8.14	0.18	3.0
14	1.64	8.54	0.19	3.2
16	1.78	8.74	0.20	3.3
18	1.78	8.74	0.20	3.3
20	1.78	8.80	0.20	3.3

values of k_4 as shown in experiments 8-14 in Table IXa, but decreased surface to volume ratio caused the k_4 values to drop as shown in Table X. The values of k_4 in Table IXa were averaged and entered into Table X under the 250°C, large furnace heading. The activation energies and pre-exponential factors are shown in Table XI.

POISONING OF THE CATALYST

The catalytic activity suddenly became very reduced when the evacuated cell was inadvertently cooled several degrees centigrade below the temperature of the manometer. In fact, the remaining reaction may be homogeneous and the catalytic activity destroyed altogether. Reactions which previously required a half hour required about ten hours after this event. It is believed that the manometer oil diffused into the reaction cell forming a layer on the fluorinated surface which inhibited the catalysis. Efforts to recover the catalyst by 400°C fluorination, by flushing with fluorine at 400°C, and by oxidation of the surface at 400°C for twenty four hours with undried air followed by fluorination failed. Further, there was no evidence of fluorine absorption by the surface after the exposure to air. This behavior is analogous to the bromination of ethylene[56], $C_2H_4 + Br_2 \longrightarrow C_2H_4Br_2$, which is catalyzed by a glass surface and which is almost completely inhibited by a coating of paraffin wax.

EQUILIBRIUM CONSTANTS

One experiment was made at 250°C with initial concentrations such that the final mixture contained all four species. The final concentrations were calculated using the equations on page 54. These were converted to pressure and equilibrium constants defined as:

$K_2 = P_2^{\infty}/P_o^{\infty}P_1^{\infty}$ and $K_4 = P_4^{\infty}/P_2^{\infty}P_1^{\infty}$ were calculated. The results are summarized in Table XIII. They are in close agreement with those in Table I and further increase ones confidence in that set of constants.

Table XIII

Equilibrium Constant Data at 250°C

P_1^{o}	=	1.53×10^{-3}	atm.
P_o^{o}	=	1.29×10^{-3}	atm.
P_o^{oo}	=	1.1×10^{-4}	atm.
P_1^{oo}	=	1.1×10^{-4}	atm.
P_2^{oo}	=	1.0×10^{-3}	atm.
P_4^{oo}	=	1.5×10^{-4}	atm.
K_2	=	8.3×10^{4}	atm.$^{-1}$
K_4	=	1.4×10^{3}	atm.$^{-1}$

DISCUSSION

Integrated Rate Expressions

The differential equation followed with excess xenon was $dC_1/dt = -k_2C_1$. This leads to:

$$C_1 = C_1^o e^{-k_2 t}$$

$$C_2 = C_1^o - C_1$$

if $C_1 = C_1^o$ and $C_2 = 0$ at $t = 0$.

The curves in Figure 13 were calculated from these equations using the appropriate constant from Table IX.

The differential equations followed, with excess fluorine, by the reactions $Xe + F_2 \xrightarrow{k_2'} XeF_2$ and $XeF_2 + F_2 \xrightarrow{k_4} XeF_4$ are:

$$dC_o/dt = -k_2'C_o$$

$$dC_2/dt = k_2'C_o - k_4C_2$$

$$dC_4/dt = k_4C_2$$

and the solutions are:

$$C_o = C_o^o e^{-k_2' t} \text{ if } C_o = C_o^o \text{ at } t = 0$$

$$C_2 = e^{-k_4 t}\left[\frac{k_2' C_o^o e^{(k_4-k_2')t} - k_2' C_o^o}{k_4-k_2'}\right] \quad \text{if } C_2 = 0 \text{ at } t = 0$$

$$C_4 = C_o^o\left[1 + \frac{k_2' e^{-k_4 t} - k_4 e^{-k_2' t}}{k_4-k_2'}\right] \quad \text{if } C_4 = 0 \text{ at } t = 0$$

$$C_1 = C_1^o - C_2 - 2C_4 \quad \text{if } C_1 = C_1^o \text{ at } t = 0$$

The curves in Figure 16 were calculated from these equations using the appropriate rate constants from Table X.

Mechanism

In general a surface reaction occurs in the following steps:[57-59]

1. Diffusion of reactants to surface
2. Adsorption of reactants at surface
3. Chemical reaction on the surface
4. Desorption of products from surface
5. Diffusion of products away from surface.

Steps 1 and 5 are usually rapid, especially at low pressures. Also the rate constants for diffusion controlled reactions have a temperature to the one half power dependence. In the work reported here the rate constants followed the Arrhenius relation. Steps 2 and 3 are included in the mechanism described below. The products xenon difluoride and xenon tetrafluoride are assumed to leave the surface immediately after formation. This is equivalent to assuming that step 4 is very rapid.

If it is assumed that molecular fluorine adsorbed on the surface of the fluorinated nickel , that the molecular fluorine dissociated on the surface forming atomic fluorine, and that the atomic fluorine reacted with gas phase xenon and xenon difluoride then the rate expressions observed by the author and those reported[33] by Baker and Fox may be derived. The chemical process may be summarized as:

$$F_{2g} \underset{\beta s\Theta}{\overset{\alpha\bar{c}C_1(1-\Theta)/4}{\rightleftharpoons}} F_{2s} \underset{bC_{Fs}^2}{\overset{as\Theta}{\rightleftharpoons}} 2F_s \qquad (1)$$

$$2F_s + Xe \xrightarrow{cC_oC_{Fs}^2} XeF_2 \qquad (2)$$

$$2F_s + XeF_2 \xrightarrow{dC_2C_{Fs}^2} XeF_4 \qquad (3)$$

The symbols used in this section are defined in Tables IX and XIV or in the text. The rate expressions are derived below and summarized in Table XV.

The rate of adsorption onto the fluorinated nickel is $\alpha\bar{c}C_1(1-\Theta)/4$ where α is a "sticking" coefficient, $\bar{c}$ is the average velocity of fluorine molecules, C_1 is the concentration of fluorine in the gas phase and Θ is the fraction of the sites which are occupied. The term $\bar{c}C_1/4$ gives the rate of collision per unit area with the surface. The term $\alpha(1-\Theta)$ is the probability that a collision will result in an adsorption. The rate of desorption is $\beta s\Theta$ where s is the concentration of fluorine on a saturated surface and β is the rate constant for desorption. The steady state equations for the adsorbed fluorine molecules and for the adsorbed fluorine atoms are:

Table XIV

Definition of Symbols

F_{2g}	=	fluorine molecules, gas phase
F_{2s}	=	fluorine molecules, surface
F_s	=	fluorine atoms, surface
C_1	=	fluorine molecule concentration, gas phase, moles per unit volume
C_{1s}	=	fluorine molecule concentration, surface, moles per unit area
C_{Fs}	=	fluorine atom concentration, surface, gram atoms per unit area
a	=	rate constant for the surface dissociation of F_{2s}
b	=	rate constant for the surface recombination of F_s
c	=	rate constant for the fluorination of xenon
d	=	rate constant for the fluorination of xenon difluoride

Table XV

Derived Rate Expressions

Rate Expressions	Observed with Initial Pressures (mm Hg) P_o	P_1
$k = as$	300	300[a]
$k_2 = \alpha \bar{c}a/4(\beta + a)$	10	1[b]
$k_2' = csa/b = csK'$	0.6	10[b]
$k_4 = dsa/b = dsK'$	0.6	10[b]

[a] B. G. Baker and P. G. Fox, Nature 204, 466 (1964).

[b] This report.

$$dC_{1s}/dt = \frac{\alpha}{4}\bar{c}C_1(1-\theta) - \beta s\theta - as\theta + bC_{Fs}^2 = 0 \tag{4}$$

$$dC_{Fs}/dt = as\theta - bC_{Fs}^2 - cC_oC_{Fs}^2 = 0 \tag{5}$$

Equation (5) may be solved for θ yielding:

$$\theta = \frac{(b + cC_o)C_{Fs}^2}{as} \tag{6}$$

Equations (4) and (5) may be added and terms collected providing the relation:

$$\frac{\alpha}{4}\bar{c}C_1 - \left(\frac{\alpha}{4}\bar{c}C_1 + \beta s\right)\theta - cC_oC_{Fs}^2 = 0 \tag{7}$$

Substituting for θ using Equation (6) yields:

$$\frac{\alpha}{4}\bar{c}C_1 - \left[\left(\frac{\alpha}{4}\bar{c}C_1 + \beta s\right)\frac{(b + cC_o)}{as} + cC_o\right] C_{Fs}^2 = 0 \tag{8}$$

The rate of production of xenon difluoride is:

$$dC_2/dt = cC_{Fs}^2C_o \tag{9}$$

If the concentration squared of fluorine atoms on the surface from Equation (8) is substituted into Equation (9), terms rearranged and expanded the result is:

$$\frac{dC_2}{dt} = \frac{c\alpha\bar{c}asC_1C_o/4}{b\beta s + (c\beta s + cas)C_o + \frac{b\alpha}{4}\bar{c}C_1 + \frac{c\alpha}{4}\bar{c}C_oC_1} \qquad (10)$$

This expression has four limits each of which is physically significant. If the concentrations of xenon and fluorine are decreased without limit

$$dC_2/dt = c\alpha\bar{c}aC_1C_o/4b\beta \qquad (11)$$

$$C_o \longrightarrow 0, \quad C_1 \longrightarrow 0$$

If the concentrations of xenon and fluorine are increased without limit

$$dC_2/dt = as \qquad (12)$$

$$C_o \longrightarrow \infty, \quad C_1 \longrightarrow \infty$$

If the concentration of xenon increases without limit and the concentration of fluorine decreases without limit

$$dC_2/dt = \left[\frac{\alpha\bar{c}a/4}{\beta + a}\right] C_1 \qquad (13)$$

$$C_o \longrightarrow \infty, \quad C_1 \longrightarrow 0$$

If the concentration of xenon decreases without limit while the concentration of fluorine increases without

limit

$$dC_2/dt = (cas/b)C_o \tag{14}$$

$$C_o \longrightarrow 0, \quad C_1 \longrightarrow \infty$$

The rates of adsorption and desorption of fluorine can not be equal under the kinetic situation, but under equilibrium conditions these rates will be equal and

$$\alpha \bar{c} C_1 (1-\theta)/4 = \beta s \theta$$

Solving this expression for θ one obtains the Langmuir isotherm.[57-59]

$$\theta = \frac{(\alpha \bar{c} C_1/4\beta s)}{1 + (\alpha \bar{c} C_1/4\beta s)}$$

For the low pressure proportional region

$$\theta = \alpha \bar{c} C_1/4\beta s$$

The concentration of fluorine molecules on the surface is:

$$C_{1F} = s\theta$$

and thus the equilibrium constant for low pressure fluorine is:

$K = C_{1F}/C_1 = \alpha\bar{c}/4\beta$

Also the equilibrium constant for fluorine molecule dissociation is equal to the ratio of constants for dissociation and recombination

$K' = a/b$

Now the rate expression at the low pressure limit, Equation (11), may be expressed as:

$dC_2/dt = cKK'C_1C_o$

For the rate constant at high fluorine and low xenon limit Equation (14) becomes:

$dC_2/dt = csK'C_o$

The other two cases, Equations 12 and 13, do not contain equilibrium constants.

The experiments of Baker and Fox,[33] described on pp. 12-13 of this report, were performed with about 300 mm each of fluorine and xenon. They found reactions of zero order with respect to each component. Hence Equation (12) must apply under those conditions and their rate constant k must equal as. This implies that the high pressure limit was achieved and that $c\alpha\bar{c}C_oC_1/4$ is much greater than

$b\beta s + (c\beta s + cas)C_o + b\alpha\bar{c}C_1/4.$

The results found in this work with much lower pressures indicate that the term containing C_1C_o is no longer dominant. The two sets of conditions under which the present study was made were one mm of fluorine with ten mm of xenon and ten mm of fluorine with 0.6 mm of xenon. The ratio of concentrations and concentration product from the conditions of Baker and Fox[33] to those of this work were:

C_1C_o	C_1	C_o	
9×10^3	300	30	(Excess xenon)
1.5×10^4	30	500	(Excess fluorine)

With changes as large as these it is not surprising that a previously dominant term may become insignificant. In addition the experimental results of Baker and Fox[33] were zero order only until half or less of the material had reacted indicating that a relatively small reduction in pressure changed the appropriate rate expression. The rate expressions found in this work were:

$$dC_2/dt = k_2C_1 \qquad \text{(Excess xenon)} \qquad (15)$$

$$dC_2/dt = k_2'C_o \qquad \text{(Excess fluorine)} \qquad (16)$$

These would imply that both the quadratic term $c\,\alpha\bar{c}C_oC_1/4$ and the constant term $b\beta s$ in Equation (10) were negligible in comparison to terms linear in

concentrations, $(c\beta s + cas)C_o$ and $b\alpha\bar{c}C_1$.

The rate expression then becomes:

$$dC_2/dt = \frac{c\alpha\bar{c}asC_1C_o/4}{(c\beta s + cas)C_o + b\alpha\bar{c}C_1/4} \qquad (17)$$

However, as may be seen in Table IXa, the range of pressures studied in this work was rather narrow especially in the case of excess fluorine where equilibrium and transparency placed lower and upper limits respectively on the pressures allowed. One may argue that the results indicated only that the experimental orders were about zero and about one in the appropriate expressions. This implies that the terms $b\beta s$ and $c\alpha\bar{c}C_oC_1/4$ may be relatively unimportant rather than negligible. In any case Equation (17) is, at least, a good approximation to the rate expression with the reactant pressures used in this work. The rate expressions (15) and (16) above indicate that the dominance of the two terms in the denominator of Equation (17) shifted within the range of conditions studied. This situation may be rationalized by rearranging (17) as follows:

$$dC_2/dt = \frac{c\frac{\alpha}{4}\bar{c}asC_o}{(c\beta s + cas)\frac{C_o}{C_1} + b\frac{\alpha}{4}\bar{c}}$$

Now the ratio C_o/C_1, which is equal to the ratio of pressures, changed from 10 or more mm of xenon/1 mm fluorine to 0.6 mm of xenon/10 or more mm fluorine. This change in ratio had a minimum value of 167 which was sufficient to produce the two limiting Equations (13) and (14) and identify the experimental rate constants as:

$$k_2 = (\alpha \bar{c} a/4)/(\beta + a) \qquad (18)$$

and

$$k_2' = cas/b = csK' \qquad (19)$$

For the reaction $F_2 + XeF_2 \longrightarrow XeF_4$ the xenon difluoride replaces the xenon in the previous discussion, the xenon tetrafluoride replaces the xenon difluoride and events on the surface remain the same. Hence the fluorination of xenon and of xenon difluoride have parallel mechanisms and the previous derivations may be repeated giving the following results:

$$dC_4/dt = \frac{d\alpha \bar{c} a s C_1 C_2/4}{b\beta s + (d\beta s + das)C_2 + \frac{b\alpha}{4}\bar{c}C_1 + \frac{d\alpha}{4}\bar{c}C_1C_2} \qquad (20)$$

$$dC_4/dt = d\alpha \bar{c} a C_1 C_2/4b\beta \qquad (21)$$

$$\text{if } C_1 \longrightarrow 0, \quad C_2 \longrightarrow 0$$

$$dC_4/dt = as \qquad (22)$$

$$\text{if } C_1 \longrightarrow \infty, \quad C_2 \longrightarrow \infty$$

$$dC_4/dt = (\alpha \bar{c}a/4)C_1/(\beta + a) \qquad (23)$$

$$\text{if } C_2 \longrightarrow \infty, \quad C_1 \longrightarrow 0$$

and

$$dC_4/dt = (das/b)C_2 \qquad (24)$$

$$\text{if } C_2 \longrightarrow 0, \quad C_1 \longrightarrow \infty$$

The experimental rate expression observed with the initial xenon pressure of 0.6 mm Hg and ten or more mm Hg of fluorine was

$$dC_4/dt = k_4C_2 \qquad (25)$$

This corresponds to the derived expression (24) which identifies k_4 as das/b which may also be expressed as dsK'. From Table X it may be seen that the ratio of k_2' to k_4 is about three. Since the enthalpy and entropy changes for these reactions are nearly the same (see Table II) and parallel reaction mechanisms are followed it seems that the major factor causing k_4 to be less than k_2' is the different geometries of the molecules of xenon and xenon difluoride.

The experimental activation energies for the rate constants were:

kcal./mole	For	Fluorine Pressure (mm Hg)
10.2[33]	k	300
12.9	k_2'	10
12.4	k_4	10
15	k_2	1

If β is negligible compared to a in the rate constant $k_2 = (\alpha \bar{c}a)/4(\beta + a)$ then $k_2 = \alpha \bar{c}/4$. The rate constant would then have a small activation energy. The experimental result above is not consistent with this conclusion. Hence β is either dominant in which case $k_2 = \alpha \bar{c}a/4\beta$ or neither term dominates. In either case the activation energy associated with the rate constant a will make an important contribution to the experimental activation energy of k_2. With this conclusion it is clear from Equations (11) thru (14) that the activation energy for the rate constant a contributes heavily to the activation energies for all of the experimental rate constants k, k_2', k_4, and k_2. The process for which a is the rate constant is the dissociation of adsorbed fluorine molecules to form adsorbed fluorine atoms. The activation energy for this process differs from that found in the gas phase because of the heats of adsorption of the two species.

It is well known that the heat of adsorption of a given species decreases as the fraction of occupied sites, θ, increases.[57-59] Now unless the magnitudes of the heats of adsorption for both fluorine molecules and two fluorine atoms decrease by exactly the same amount the energy of activation of the dissociation on the surface will be a function of θ and, hence, a function of the pressure of fluorine in the gas phase. It is likely that the magnitude of the heat of adsorption of fluorine molecules decreases more rapidly than that of the fluorine atoms. The bond of a fluorine atom to the surface is expected to be more nearly like a covalent chemical bond and hence about constant. The bond of a fluorine molecule is expected to be weaker and, thus, more strongly effected by surface hetergeneity. The sites yielding the strongest bonds with molecular fluorine are occupied first followed by those sites yielding decreasing bond energies as θ increases. This model leads to the conclusion that the energy of activation for fluorine molecule dissociation on the surface and for the experimental rate constants should decrease as the pressure of fluorine increases. This trend is clearly present in the values of k_2, k_2' and k listed above. The experimental activation energies for k_2' and k_4 were essentially equal as were the fluorine pressures used. The expression for the rate constant in the case of Baker and Fox is $k = \underline{a}s$. Since s is considered

to be independent of the temperature the experimental activation energy observed, 10.2 kcal./mole, is equal to the activation energy of fluorine dissociation on the fluorinated nickel surface at 300 mm Hg fluorine in the gas phase. The other experimental activation energies are composites nearly but not completely dominated by the unknown activation energies of fluorine dissociation at their particular pressures.

The qualitative description (pp. 10-11) of the kinetics of xenon-fluorine reactions monitored by infrared radiation[3,30] does not seem to fit the pattern described here. However, no pressures were given making a comparison impossible.

Miscellaneous

If further studies of the catalyzed xenon-fluorine reactions in fluorinated nickel are made the hot cell must be protected from the manometer oil. A bellows manometer would accomplish this but with a loss of sensitivity in the pressure measurement. Perhaps a cold trap between the manometer and the hot cell would solve the problem without this loss of sensitivity. On the other hand if one wished to study the homogeneous reactions of the elements perhaps the catalysis could be prevented by exposing the reaction cell to the halogenated alkane immediately before each experiment. This might be useful

in photochemical as well as thermal reactions.

Extending the investigation of reactions involving xenon tetrafluoride to 400°C requires the measurement of absorption coefficients to that temperature. Even if the hexafluoride continues to be absent much higher pressures are required. From Table I it can be seen that the ratio $P_4/P_2 = 4.86 \times P_1$ at 400°C. Thus for this ratio to be greater than ten, P_1 must be greater than two atmospheres. At such concentrations, however, fluorine is opaque in the present apparatus. By reducing the length of the cell to fifteen centimeters and changing the wave length to 4000 Å two orders of magnitude higher pressures (about 4 atm.) of fluorine will be transparent, but larger end corrections will result. The problem of condensation will also be greater. Cooling the windows to about 200°C rather than room temperature would solve this problem (see Figure 2). These innovations would also allow the extention of the optical measurement of equilibrium constants.

Another useful extention of the work would be to synthesize or obtain from another source a sample of pure xenon hexafluoride and measure its near ultra-violet absorption spectrum. Only qualitative information is presently available.[1,19]

ACKNOWLEDGMENTS

The author wishes to thank Professor Harold S. Johnston for his instruction, advice and patience. The lively discussions and good humor of the members of the group made the past three years very enjoyable as well as professionally valuable. Financial support from the National Science Foundation, the United States Atomic Energy Commission through the Inorganic Materials Research Division of the Lawrence Radiation Laboratory, and the Reactor Chemistry Division of the Oak Ridge National Laboratory is gratefully acknowledged. A very special thanks goes to my wife for her tolerance, encouragement, and extensive secretarial services.

APPENDIX

Kinetic Data Supporting Text

List of Appendix Tables

Table	Wave Lengths (Å)		Temperature (°C)	Furnace Diameter (cm)	Excess Reactant
IA	2518		190	1.59	Xe
IIA	2518		190	1.59	Xe
IIIA	2518		190	1.59	Xe
IVA	2518		225	1.59	Xe
VA	2518		250	1.59	Xe
VIA	2518		250	1.59	Xe
VIIA	2518		250	1.59	Xe
VIIIA	2518		250	6.28	Xe
IXA	2518		250	6.28	Xe
XA	2518		250	6.28	Xe
XIA	2618		250	6.28	Xe
XIIA	2518		290	6.28	Xe
XIIIA	2518		330	6.28	Xe
XIVA	2518		400	6.28	Xe
XVA	2618		400	6.28	Xe
XVIA	2518	2768	190	1.59	F_2
XVIIA	2518	2768	190	1.59	F_2
XVIIIA	2518	2768	190	1.59	F_2
XIXA	2518	2768	225	1.59	F_2
XXA	2518	2768	250	1.59	F_2
XXIA	2518	2768	250	1.59	F_2
XXIIA	2518	2768	250	1.59	F_2

APPENDIX

Kinetic Data Supporting Text

Appendix Tables (Contd.)

Table	Wave Lengths (Å)		Temperature (°C)	Furnace Diameter (cm)	Excess Reactant
XXIIIA	2518	2768	190	6.28	F_2
XXIVA	2518	2768	190	6.28	F_2
XXVA	2518	2768	190	6.28	F_2
XXVIA	2518	2768	225	6.28	F_2
XXVIIA	2518	2768	250	6.28	F_2
XXVIIIA	2518	2768	250	6.28	F_2
XXIXA	2518	2768	250	6.28	F_2
XXXA	2618	2868	250	6.28	F_2

Summary of Rate Constants in Appendix

Table	Temperature (°C)	Furnace Diameter (cm)	Initial Pressures (mm Hg)			Constants $(sec^{-1}) \times 10^3$		
			F_2	Xe	Ar	k_2	k_2'	k_4
IA	190	1.59	1.12	9.17	125	2.9		
IIA	190	1.59	1.00	9.19	295	3.3		
IIIA	190	1.59	1.03	20.1	125	2.9		
IVA	225	1.59	1.02	10.1	105	9.8		
VA	250	1.59	0.926	14.7	22.9	24		
VIA	250	1.59	0.912	14.7	3.79	22		
VIIA	250	1.59	0.919	54.8	3.94	22		
VIIIA	250	6.28	1.08	13.0	15	2.0		
IXA	250	6.28	1.17	13.3	96	1.9		
XA	250	6.28	1.18	25.3	98	2.0		
XIA	250	6.28	1.05	13.2	16	1.9		
XIIA	290	6.28	1.11	13.2	95	4.3		
XIIIA	330	6.28	1.06	12.9	92	12		
XIVA	400	6.28	1.08	13.1	93	38		
XVA	400	6.28	1.09	13.0	96	37		
XVIA	190	1.59	10.1	0.585	149		30	10.0
XVIIA	190	1.59	10.3	0.592	303		29	9.8
XVIIIA	190	1.59	19.7	0.579	153		27	10.2

Summary (Contd.)

Table	Temperature (°C)	Furnace Diameter (cm)	Initial Pressures (mm Hg)			Constants $(sec^{-1}) \times 10^3$		
			F_2	Xe	Ar	k_2	k_2'	k_4
XIXA	225	1.59	10.1	0.580	153		72	25
XXA	250	1.59	10.3	0.586	150		150	48
XXIA	250	1.59	10.1	0.578	153		140	53
XXIIA	250	1.59	20.1	0.588	147		160	50
XXIIIA	190	6.28	10.0	0.580	151		1.8	0.68
XXIVA	190	6.28	10.2	0.593	299		2.2	0.72
XXVA	190	6.28	20.3	0.587	145		2.0	0.66
XXVIA	225	6.28	10.4	0.591	152		6.2	1.8
XXVIIA	250	6.28	10.1	0.581	148		9.7	3.2
XXVIIIA	250	6.28	10.0	0.590	300		10.4	3.0
XXIXA	250	6.28	19.8	0.573	151		10.3	3.1
XXXA	250	6.28	10.2	0.585	150		9.7	2.8

Table IA

XeF_2 Formation in Excess Xe

Time (min.)	I^o/I	Concentrations (moles/cc. x 10^8) C_1	C_2	$\log(C_1^o/C_1)$
0		3.89	0.00	0.000
1	1.113	3.50	0.39	0.045
2	1.231	2.82	1.07	0.140
3	1.293	2.49	1.40	0.194
4	1.376	2.07	1.82	0.274
5	1.438	1.77	2.12	0.342
6	1.488	1.55	2.34	0.400
7	1.542	1.31	2.58	0.473
8	1.600	1.06	2.83	0.565
9	1.620	0.96	2.92	0.608
10	1.662	0.80	3.09	0.685
12	1.730	0.53	3.36	0.862
14	1.778	0.35	3.54	1.045
16	1.803	0.26	3.63	1.180
18	1.829	0.16	3.73	1.383
20	1.855	0.07	3.82	1.770

Initial Pressures	F_2	Xe	Ar
(mm Hg)	1.12	9.17	125

Temperature 190°C Furnace Diameter 1.59 cm. Wave Length 2518 Å

Table IIA

XeF_2 Formation in Excess Xe

Time (min.)	I^o/I	Concentrations (moles/cc. x 10^8) C_1	C_2	$\log(C_1^o/C_1)$
0		3.46	0.00	0.000
1	1.098	2.82	0.64	0.089
2	1.175	2.45	1.01	0.150
3	1.241	2.22	1.24	0.183
4	1.288	1.96	1.50	0.247
5	1.367	1.53	1.93	0.354
6	1.411	1.31	2.15	0.422
7	1.457	1.18	2.38	0.467
8	1.523	0.76	2.70	0.658
9	1.558	0.60	2.86	0.761
10	1.595	0.43	3.03	0.906
12	1.614	0.35	3.11	0.995
14	1.634	0.26	3.20	1.124
16	1.675	0.09	3.37	1.584
18	1.675	0.09	3.37	1.584
20	1.675	0.09	3.37	1.584

Initial Pressures	F_2	Xe	Ar
(mm Hg)	1.00	9.19	295

Temperature 190°C Furnace Diameter 1.59 cm. Wave Length 2518 Å

Table IIIA

XeF_2 Formation in Excess Xe

Time (min.)	I^o/I	Concentrations (moles/cc. x 10^8) C_1	C_2	$\log(C_1^o/C_1)$
0		3.59	0.00	0.000
1	1.092	3.33	0.26	0.033
2	1.202	2.76	0.83	0.114
3	1.259	2.48	1.11	0.161
4	1.338	2.12	1.47	0.229
5	1.408	1.82	1.77	0.295
6	1.486	1.50	2.09	0.379
7	1.551	1.24	2.35	0.462
8	1.621	0.98	2.61	0.564
9	1.672	0.79	2.80	0.655
10	1.698	0.70	2.89	0.709
12	1.783	0.41	3.18	0.941
14	1.845	0.21	3.38	1.239
16	1.877	0.11	3.49	1.534
18	1.877	0.11	3.49	1.534
20	1.911	0.00	3.59	

Initial Pressures	F_2	Xe	Ar
(mm Hg)	1.03	20.1	125

Temperature 190°C Furnace Diameter 1.59 cm. Wave Length 2518 Å

Table IVA

XeF_2 Formation in Excess Xe

Time (sec.)	I^o/I	Concentrations (moles/cc x 10^8)		$\log(C_1^o/C_1)$
		C_1	C_2	
0		3.10	0.00	0.000
20	1.143	2.55	0.55	0.088
40	1.224	2.10	1.00	0.172
60	1.322	1.72	1.38	0.261
100	1.415	1.17	1.93	0.426
140	1.491	0.76	2.34	0.615
180	1.556	0.53	2.57	0.769

Initial Pressures	F_2	Xe	Ar
(mm Hg)	1.02	10.1	105

Temperature 225°C. Furnace Diameter 1.59 cm Wave Length 2518 Å

Table VA

XeF_2 Formation in Excess Xe

Time (sec.)	I^o/I	Concentrations (moles/cc. x 10^8) C_1	C_2	$\log(C_1^o/C_1)$
0		2.84	0.00	0.000
10	1.129	2.41	0.44	0.072
20	1.263	1.84	1.00	0.188
30	1.380	1.39	1.45	0.310
40	1.490	1.10	1.74	0.412
50	1.461	1.00	1.84	0.453
70	1.585	0.69	2.15	0.615

Initial Pressures	F_2	Xe	Ar
(mm Hg)	0.926	14.7	22.9

Temperature 250°C. Furnace Diameter 1.59 cm. Wave Length 2518 Å

Table VIA

XeF_2 Formation in Excess Xe

Time (sec.)	I^o/I	Concentrations (moles/cc. x 10^8)		$\log(C_1^o/C_1)$
		C_1	C_2	
0		2.80	0.00	0.000
10	1.123	2.43	0.37	0.061
20	1.253	1.94	0.86	0.159
30	1.352	1.59	1.21	0.246
40	1.451	1.27	1.53	0.306
50	1.526	1.05	1.75	0.426
70	1.676	0.62	2.18	0.654

Initial Pressures	F_2	Xe	Ar
(mm Hg)	0.912	14.7	3.79

Temperature 250°C. Furnace Diameter 1.59 cm Wave Length 2518 Å

Table VIIA

XeF_2 Formation in Excess Xe

Time (sec.)	I^o/I	Concentrations (moles/cc. x 10^8)		$\log(C_1^o/C_1)$
		C_1	C_2	
0		2.82	0.00	0.000
10	1.125	2.42	0.40	0.062
20	1.262	1.90	0.92	0.174
30	1.374	1.46	1.36	0.288
40	1.463	1.17	1.65	0.384
50	1.511	1.04	1.78	0.436
70	1.647	0.68	2.14	0.620

Initial Pressures	F_2	Xe	Ar
(mm Hg)	0.919	54.8	3.94

Temperature 250°C. Furnace Diameter 1.59 cm Wave Length 2518 Å

Table VIIIA

XeF_2 Formation in Excess Xe

Time (min.)	I^o/I	Concentrations (moles/cc. x 10^8) C_1	C_2	$\log(C_1^o/C_1)$
0		3.33	0.00	0.000
1	1.076	3.12	0.21	0.028
2	1.148	2.69	0.64	0.092
3	1.211	2.34	0.99	0.153
4	1.260	2.08	1.25	0.204
5	1.314	1.80	1.53	0.266
6	1.348	1.64	1.69	0.309
7	1.396	1.41	1.93	0.375
8	1.435	1.22	2.11	0.435
9	1.462	1.10	2.23	0.481
10	1.505	0.91	2.42	0.563
12	1.550	0.72	2.61	0.667
14	1.598	0.52	2.82	0.811
16	1.632	0.38	2.95	0.946
18	1.649	0.31	3.02	1.033
20	1.685	0.17	3.16	1.300

Initial Pressures	F_2	Xe	Ar
(mm Hg)	1.08	13.0	15

Temperature 250°C Furnace Diameter 6.28 cm Wave Length 2518 Å

Table IXA

XeF_2 Formation in Excess Xe

Time (min.)	I^o/I	Concentrations (moles/cc. x 10^8) C_1	C_2	$\log(C_1^o/C_1)$
0		3.60	0.00	0.000
1	1.076	3.40	0.20	0.025
2	1.140	3.00	0.60	0.079
3	1.202	2.64	0.96	0.135
4	1.281	2.20	1.41	0.214
5	1.325	1.96	1.64	0.264
6	1.360	1.78	1.82	0.306
7	1.409	1.54	2.06	0.369
8	1.449	1.34	2.26	0.429
9	1.490	1.15	2.45	0.496
10	1.520	1.01	2.59	0.552
12	1.598	0.67	2.93	0.730
14	1.649	0.45	3.15	0.903
16	1.685	0.30	3.30	1.079
18	1.722	0.15	3.45	1.380
20	1.722	0.15	3.45	1.380

Initial Pressures	F_2	Xe	Ar
(mm Hg)	1.17	13.3	96

Temperature 250°C. Furnace Diameter 6.28 cm Wave Length 2518 Å

Table XA

XeF_2 Formation in Excess Xe

Time (min.)	I^o/I	Concentrations (moles/cc. x 10^8) C_1	C_2	$\log(C_1^o/C_1)$
0		3.63	0.00	0.000
1	1.081	3.39	0.24	0.032
2	1.138	2.98	0.65	0.088
3	1.210	2.65	0.98	0.140
4	1.285	2.25	1.38	0.210
5	1.319	1.94	1.69	0.274
6	1.361	1.79	1.84	0.310
7	1.419	1.60	2.03	0.358
8	1.451	1.32	2.31	0.445
9	1.499	1.14	2.49	0.506
10	1.516	0.99	2.64	0.567
12	1.601	0.69	2.94	0.724
14	1.643	0.45	3.18	0.909
16	1.692	0.29	3.34	1.100
18	1.719	0.16	3.47	1.358
20	1.729	0.15	3.48	1.386

Initial Pressures	F_2	Xe	Ar
(mm Hg)	1.18	25.3	98

Temperature 250°C. Furnace Diameter 6.28 cm Wave Length 2518 Å

Table XIA

XeF_2 Formation in Excess Xe

Time (min.)	I^o/I	Concentrations (moles/cc. x 10^8) C_1	C_2	$\log(C_1^o/C_1)$
0		3.23	0.00	0.000
1	1.052	3.02	0.21	0.032
2	1.092	2.60	0.63	0.095
3	1.130	2.25	0.98	0.160
4	1.163	2.01	1.22	0.213
5	1.195	1.72	1.51	0.276
6	1.219	1.59	1.64	0.311
7	1.248	1.46	1.77	0.347
8	1.261	1.18	2.05	0.424
9	1.287	1.07	2.16	0.482
10	1.312	0.89	2.34	0.557
12	1.335	0.70	2.53	0.666
14	1.360	0.51	2.72	0.813
16	1.387	0.36	2.87	0.956
18	1.392	0.30	2.93	1.041
20	1.422	0.15	3.08	1.345

Initial Pressures	F_2	Xe	Ar
(mm Hg)	1.05	13.2	16

Temperature 250°C. Furnace Diameter 6.28 cm Wave Length 2618 Å

Table XIIA

XeF_2 Formation in Excess Xe

Time (min.)	I^o/I	Concentrations (moles/cc x 10^8) C_1	C_2	$\log(C_1^o/C_1)$
0		3.25	0.00	0.000
1	1.222	2.78	0.47	0.071
2	1.383	1.97	1.28	0.197
3	1.451	1.59	1.66	0.312
4	1.498	1.30	1.95	0.400
5	1.560	0.94	2.31	0.539
6	1.603	0.78	2.47	0.622
7	1.650	0.62	2.63	0.720
8	1.693	0.42	2.83	0.894
9	1.712	0.34	2.91	0.980
10	1.733	0.25	3.00	1.120
12	1.761	0.16	3.09	1.300
14	1.770	0.11	3.14	1.465

Initial Pressures	F_2	Xe	Ar
(mm Hg)	1.11	13.2	95

Temperature 290°C. Furnace Diameter 6.28 cm Wave Length 2518 Å

Table XIIIA

XeF_2 Formation in Excess Xe

Time (sec.)	I^o/I	Concentrations (moles/cc x 10^8)		$\log(C_1^o/C_1)$
		C_1	C_2	
0		3.04	0.00	0.000
20	1.276	2.51	0.53	0.085
40	1.341	1.99	1.05	0.188
60	1.429	1.53	1.51	0.300
80	1.504	1.14	1.90	0.391
100	1.542	0.99	2.05	0.489
120	1.619	0.64	2.40	0.617
150	1.713	0.40	2.63	0.883
190	1.868	0.31	2.73	0.989

Initial Pressures	F_2	Xe	Ar
(mm Hg)	1.06	12.9	92

Temperature 330°C. Furnace Diameter 6.28 cm Wave Length 2518 Å

Table XIVA

XeF_2 Formation in Excess Xe

Time (sec.)	I^o/I	Concentrations (moles/cc x 10^8) C_1	C_2	$\log(C_1^o/C_1)$
0		2.69	0.00	0.000
10	1.214	2.16	0.53	0.105
20	1.407	1.46	1.23	0.266
30	1.547	1.01	1.67	0.427
40	1.651	0.70	1.99	0.586
50	1.760	0.49	2.20	0.747
60	1.831	0.31	2.38	0.907
70	1.906	0.23	2.46	1.07
80	1.936	0.16	2.53	1.23

Initial Pressures	F_2	Xe	Ar
(mm Hg)	1.08	13.1	93

Temperature 400°C. Furnace Diameter 6.28 cm Wave Length 2518 Å

Table XVA

XeF_2 Formation in Excess Xe

Time (sec.)	I^o/I	Concentrations (moles/cc x 10^8) C_1	C_2	$\log(C_1^o/C_1)$
0		2.71	0.00	0.000
10	1.154	2.17	0.55	0.099
20	1.317	1.48	1.22	0.261
30	1.397	1.02	1.69	0.431
40	1.471	0.71	2.01	0.582
50	1.550	0.48	2.36	0.752
60	1.591	0.33	2.49	0.913
70	1.636	0.25	2.49	1.03
80	1.656	0.16	2.54	1.22

Initial Pressures	F_2	Xe	Ar
(mm Hg)	1.09	13.0	96

Temperature 400°C. Furnace Diameter 6.28 cm Wave Length 2618 Å

Table XVIA

XeF_4 Formation in Excess F_2

Time (min.)	I^o/I (2518 Å)	I^o/I (2768 Å)	Concentrations (moles/cc x 10^8) C_4	C_2	C_o	$\log(C_o^o/C_o)$
0	1.658	1.815	0.00	0.00	2.04	0.00
0.5	2.344	2.136	0.27	0.80	0.98	0.32
1	3.033	2.463	0.58	1.12	0.33	0.79
2	3.415	2.621	1.09	0.93		
3	3.826	2.814	1.44	0.59		
4	4.241	3.039	1.70	0.32		
5	4.639	3.258	1.94	0.09		
6	4.724	3.344	2.03	0.02		

Initial Pressures	F_2	Xe	Ar
(mm Hg)	10.1	0.585	149

Temperature 190°C. Furnace Diameter 1.59 cm

Table XVIIA

XeF_4 Formation in Excess F_2

Time (min.)	I^o/I (2518 Å)	I^o/I (2768 Å)	Concentrations (moles/cc x 10^8) C_4	C_2	C_o	$\log(C_o^o/C_o)$
0	1.663	1.802	0.00	0.00	2.05	0.00
0.5	2.352	2.129	0.28	0.81	0.96	0.35
1	3.045	2.473	0.55	1.03	0.36	0.76
2	3.404	2.644	1.11	0.92		
3	3.849	2.836	1.42	0.63		
4	4.261	3.028	1.71	0.34		
5	4.618	3.234	1.98	0.08		
6	4.743	3.347	2.00	0.04		

Initial Pressures (mm Hg)	F_2	Xe	Ar
	10.3	0.592	303

Temperature 190°C. Furnace Diameter 1.59 cm

Table XVIIIA

XeF_4 Formation in Excess F_2

Time (min.)	I^o/I (2518 Å)	I^o/I (2768 Å)	Concentrations (moles/cc x 10^8) C_4	C_2	C_o	$\log(C_o^o/C_o)$
0	2.421	2.995	0.00	0.00	2.02	0.00
0.5	3.036	3.464	0.33	0.88	0.80	0.41
1.0	3.787	3.781	0.54	1.06	0.41	0.70
2	4.842	4.429	1.03	0.95		
3	5.833	5.048	1.45	0.61		
4	6.706	5.256	1.71	0.30		
5	6.484	5.402	1.93	0.08		
6	7.033	5.577	2.01	0.01		

Initial Pressures	F_2	Xe	Ar
(mm Hg)	19.7	0.579	153

Temperature 190°C. Furnace Diameter 1.59 cm

Table XIXA

XeF_4 Formation in Excess F_2

Time (sec.)	I^o/I (2518 Å)	I^o/I (2768 Å)	Concentrations (moles/cc x 10^8) C_4	C_2	C_o	$\log(C_o^o/C_o)$
0	1.632	1.789	0.00	0.00	1.91	0.00
20	2.217	2.032	0.48	1.00	0.41	0.67
40	2.754	2.259	0.85	0.99	0.09	1.33
60	3.321	2.662	1.21	0.70		
80	3.736	2.758	1.48	0.42		
100	4.201	2.908	1.60	0.31		
120	4.313	3.041	1.81	0.09		
140	4.417	3.111	1.90	0.01		

Initial Pressures (mm Hg)	F_2	Xe	Ar
	10.1	0.580	153

Temperature 225°C. Furnace Diameter 1.59 cm

Table XXA

XeF_4 Formation in Excess F_2

Time (sec.)	I^o/I (2518 Å)	I^o/I (2768 Å)	Concentrations (moles/cc x 10^8) C_4	C_2	C_o	$\log(C_o^o/C_o)$
0	1.491	1.653	0.00	0.00	1.81	0.00
5	1.843	1.811	0.20	0.76	0.84	0.33
10	2.152	1.994	0.41	0.93	0.44	0.66
20	2.814	2.312	0.82	0.93		
30	3.215	2.448	1.13	0.66		
40	3.562	2.727	1.36	0.44		
60	4.201	2.875	1.70	0.06		
80	4.313	3.053	1.81	0.03		

Initial Pressures (mm Hg)	F_2	Xe	Ar
	10.3	0.586	150

Temperature 250°C. Furnace Diameter 1.59 cm

Table XXIA

XeF_4 Formation in Excess F_2

Time (sec.)	I^o/I (2518 Å)	I^o/I (2768 Å)	Concentrations (moles/cc x 10^8) C_4	C_2	C_o	$\log(C_o^o/C_o)$
0	1.473	1.633	0.00	0.00	1.79	0.00
5	1.864	1.834	0.22	0.71	0.86	0.32
10	2.155	1.992	0.51	0.90	0.38	0.68
20	2.793	2.291	0.78	0.92		
30	3.236	2.468	1.10	0.68		
40	3.561	2.724	1.37	0.42		
60	4.224	2.896	1.74	0.07		
80	4.293	3.038	1.78	0.02		

Initial Pressures (mm Hg)	F_2	Xe	Ar
	10.1	0.578	153

Temperature 250°C. Furnace Diameter 1.59 cm

Table XXIIA

XeF_4 Formation in Excess F_2

Time (sec.)	I^o/I (2518 Å)	I^o/I (2768 Å)	Concentrations (moles/cc x 10^8) C_4	C_2	C_o	$\log(C_o^o/C_o)$
0	2.213	2.721	0.00	0.00	1.83	0.00
5	2.724	3.034	0.17	0.73	0.93	0.30
10	3.851	3.606	0.58	0.89	0.36	0.70
20	4.273	3.829	0.79	0.94		
30	4.889	4.133	1.14	0.69		
40	5.565	4.531	1.42	0.41		
60	6.429	4.909	1.78	0.05		
80	6.481	5.046	1.82	0.01		

Initial Pressures (mm Hg)	F_2	Xe	Ar
	20.1	0.588	147

Temperature 250°C. Furnace Diameter 1.59 cm

Table XXIIIA

XeF_4 Formation in Excess F_2

Time (min.)	I^o/I (2518 Å)	I^o/I (2768 Å)	Concentrations (moles/cc x 10^8) C_4	C_2	C_o	$\log(C_o^o/C_o)$
0	1.661	1.801	0.00	0.00	2.03	0.00
5	2.039	1.959	0.16	0.86	0.99	0.31
10	3.041	2.420	0.38	0.99	0.67	0.49
20	3.263	2.503	0.85	1.19		
40	3.872	2.862	1.36	0.68		
60	4.239	3.043	1.69	0.32		
80	4.743	3.309	1.98	0.04		

Initial Pressures (mm Hg)	F_2	Xe	Ar
	10.0	0.580	151

Temperature 190°C. Furnace Diameter 6.28 cm

Table XXIVA

XeF_4 Formation in Excess F_2

Time (min.)	I^o/I (2518 Å)	I^o/I (2768 Å)	Concentrations (moles/cc x 10^8) C_4	C_2	C_o	$\log(C_o^o/C_o)$
0	1.681	1.821	0.00	0.00	2.05	0.00
5	2.018	1.945	0.18	0.66	1.21	0.23
10	3.062	2.406	0.40	1.11	0.54	0.58
20	3.281	2.515	0.87	1.18		
40	3.899	2.888	1.40	0.65		
60	4.214	3.023	1.65	0.40		
80	4.703	3.299	2.01	0.04		

Initial Pressures (mm Hg)	F_2	Xe	Ar
	10.2	0.593	299

Temperature 190°C. Furnace Diameter 6.28 cm

Table XXVA

XeF_4 Formation in Excess F_2

Time (min.)	I^o/I (2518 Å)	I^o/I (2768 Å)	Concentrations (moles/cc x 10^8) C_4	C_2	C_o	$\log(C_o^o/C_o)$
0	2.438	2.986	0.00	0.00	2.04	0.00
5	2.861	3.329	0.17	0.74	1.13	0.26
10	3.838	3.831	0.41	1.05	0.58	0.55
20	4.842	4.462	0.88	1.16		
40	5.863	5.083	1.35	0.69		
60	6.474	5.446	1.62	0.42		
80	7.029	5.651	2.00	0.04		

Initial Pressures (mm Hg)	F_2	Xe	Ar
	20.3	0.587	145

Temperature 190°C. Furnace Diameter 6.28 cm

Table XXVIA

XeF_4 Formation in Excess F_2

Time (min.)	I^o/I (2518 Å)	I^o/I (2768 Å)	Concentrations (moles/cc x 10^8) C_4	C_2	C_o	$\log(C_o^o/C_o)$
0	1.621	1.759	0.00	0.00	1.93	0.00
2	1.913	1.961	0.22	0.83	0.87	0.35
4	2.204	2.023	0.47	1.02	0.43	0.65
8	2.719	2.234	0.87	0.99		
12	3.327	2.661	1.22	0.70		
20	4.253	2.956	1.67	0.21		
30	4.445	3.107	1.93	0.00		

Initial Pressures (mm Hg)	F_2	Xe	Ar
	10.4	0.591	152

Temperature 225°C. Furnace Diameter 6.28 cm

Table XXVIIA

XeF_4 Formation in Excess F_2

Time (min.)	I^o/I (2518 Å)	I^o/I (2768 Å)	Concentrations (moles/cc x 10^8) C_4	C_2	C_o	$\log(C_o^o/C_o)$
0	1.490	1.651	0.00	0.00	1.79	0.00
0.5	1.596	1.704	0.06	0.28	1.43	0.10
1	1.780	1.797	0.16	0.77	0.86	0.31
1.5	1.984	1.896	0.30	0.82	0.68	0.42
2	2.086	1.945	0.36	0.84	0.59	0.48
2.5	2.201	2.018	0.44	0.88	0.46	0.59
3	2.317	2.088	0.51	0.92	0.36	0.70
3.5	2.500	2.162	0.63	0.95	0.21	0.94
4	2.561	2.185	0.67	0.96	0.16	1.05
5	2.808	2.306	0.81	1.00		
6	3.042	2.383	1.00	0.79		
7	3.174	2.424	1.09	0.72		
8	3.318	2.509	1.20	0.59		
9	3.476	2.600	1.30	0.51		
10	3.561	2.717	1.36	0.43		
12	3.744	2.769	1.47	0.33		

Initial Pressures	F_2	Xe	Ar
(mm Hg)	10.1	0.581	148

Temperature 250°C. Furnace Diameter 6.28 cm

Table XXVIIA (Contd.)

XeF_4 Formation in Excess F_2

Time (min.)	I^o/I (2518 Å)	I^o/I (2768 Å)	Concentrations moles/cc x 10^8 C_4	C_2	C_o	$\log(C_o^o/C_o)$
14	4.056	2.843	1.64	0.19		
16	4.294	2.900	1.78	0.02		
18	4.294	2.959	1.78	0.02		
20	4.294	3.042	1.78	0.02		

Table XXVIIIA

XeF_4 Formation in Excess F_2

Time (min.)	I^o/I (2518 Å)	I^o/I (2768 Å)	Concentrations (moles/cc. x 10^8) C_4	C_2	C_o	$\log(C_o^o/C_o)$
0	1.476	1.641	0.00	0.00	1.82	0.00
1	1.793	1.791	0.14	0.78	0.87	0.30
2	2.090	1.950	0.35	0.86	0.57	0.46
3	2.309	2.075	0.49	0.92	0.34	0.68
4	2.550	2.190	0.67	0.95	0.14	1.09
5	2.813	2.301	0.79	1.01		
6	3.052	2.387	0.98	0.80		
7	3.163	2.414	1.11	0.73		
8	3.321	2.513	1.20	0.61		
9	3.466	2.603	1.29	0.50		
10	3.570	2.721	1.38	0.44		
12	3.754	2.759	1.46	0.31		
14	4.052	2.836	1.66	0.20		
16	4.280	2.902	1.76	0.06		
18	4.297	2.940	1.82	0.00		
20	4.289	3.031	1.80	0.02		

Initial Pressures	F_2	Xe	Ar
(mm. Hg)	10.0	0.590	300
Temperature	250°C	Furnace Diameter	6.28 cm.

Table XXIXA

XeF_4 Formation in Excess F_2

Time (min.)	I^o/I (2518 Å)	I^o/I (2768 Å)	Concentrations (moles/cc x 10^8) C_4	C_2	C_o	$\log(C_o^o/C_o)$
0	2.201	2.722	0.00	0.00	1.80	0.00
1	2.679	2.985	0.17	0.76	0.90	0.30
2	3.117	3.247	0.38	0.83	0.56	0.51
3	3.442	3.444	0.49	0.90	0.39	0.67
4	3.803	3.649	0.67	0.97	0.15	1.08
5	4.196	3.821	0.79	0.90		
6	4.545	3.969	1.00	0.82		
7	4.721	4.007	1.11	0.71		
8	4.958	4.172	1.20	0.60		
9	5.161	4.323	1.29	0.48		
10	5.308	4.526	1.36	0.45		
12	5.589	4.588	1.46	0.30		
14	6.034	4.711	1.65	0.22		
16	6.387	4.828	1.75	0.05		
18	6.405	4.881	1.78	0.02		
20	6.392	5.025	1.81	0.00		

Initial Pressures	F_2	Xe	Ar
(mm Hg)	19.8	0.573	151

Temperature 250°C. Furnace Diameter 6.28 cm

Table XXXA

XeF_4 Formation in Excess F_2

Time (min.)	I^o/I (2618 Å)	I^o/I (2868 Å)	Concentrations (moles/cc x 10^8) C_4	C_2	C_o	$\log(C_o^o/C_o)$
0	1.551	1.731	0.00	0.00	1.81	0.00
1	1.837	1.883	0.06	0.75	1.00	0.26
2	2.113	2.032	0.44	0.86	0.51	0.55
3	2.335	2.104	0.53	0.94	0.34	0.73
4	2.564	2.189	0.67	0.98	0.16	1.06
5	2.892	2.258	0.78	1.03		
6	3.226	2.317	1.04	0.77		
7	3.429	2.415	1.07	0.74		
8	3.638	2.516	1.25	0.57		
9	3.776	2.614	1.28	0.53		
10	3.912	2.712	1.40	0.41		
12	4.234	2.803	1.46	0.35		
14	4.565	2.901	1.64	0.17		
16	4.913	2.977	1.79	0.02		
18	5.277	3.039	1.81	0.00		
20	5.651	3.098	1.80	0.01		

Initial Pressures	F_2	Xe	Ar
(mm Hg)	10.2	0.585	150

Temperature 250°C. Furnace Diameter 6.28 cm

BIBLIOGRAPHY

1. J. G. Malm, H. Selig, J. Jortner, and S. A. Rice, Chem. Rev. 65, 199 (1965).

2. Herbert H. Hyman, ed., Noble-Gas Compounds, University of Chicago Press, Chicago, Ill., 1963.

3. D. F. Smith, ibid. p. 39.

4. H. H. Claasen, J. G. Malm, and H. Selig, ibid. p. 31.

5. H. H. Claasen, H. Selig, and J. G. Malm, J. Am. Chem. Soc. 84, 3593 (1962).

6. C. L. Chernick, Noble-Gas Compounds, University of Chicago Press, Chicago, Ill., 1963, p. 35.

7. B. Weinstock, E. E. Weaver, and C. P. Knop, presented at 148th National Meeting of the American Chemical Society, Chicago, Ill., Sept. 1964.

8. B. Weinstock, E. E. Weaver, and C. P. Knop, Noble-Gas Compounds, University of Chicago Press, Chicago, Ill., 1963, p. 50.

9. A. G. Streng, A. D. Kirshenbaum, L. V. Streng, and A. V. Grosse, ibid. p. 73.

10. H. G. Gale and G. S. Monk, Phys. Rev. 29, 211 (1927).

11. H. von Wartenberg and J. Taylor, Nachr. Ges. Wiss. Göttingen Math.-physik Classe 1, 119 (1930).

12. H. von Wartenberg, G. Sprenger and J. Taylor, Z. physik. Chem. Bodenstein-Festband 61, (1931).

13. M. Bodenstein and H. Jockusch, Z. anorg. allgem. Chem., 231, 24 (1937).

14. R. K. Steunenberg and R. C. Vogel, J. Am. Chem. Soc. 78, 901 (1956).

15. J. Jortner, E. G. Wilson, and S. A. Rice, Noble-Gas Compounds, University of Chicago Press, Chicago, Ill., 1963, p. 358.

16. E. S. Pysh, J. Jortner, and S. A. Rice, J. Chem. Phys. 40, 2018 (1964).

17. E. G. Wilson, J. Jortner, and S. A. Rice, J. Am. Chem. Soc. 85, 813 (1963).

18. J. Jortner, E. G. Wilson, and S. A. Rice, ibid. 815 (1963).

19. J. G. Malm, I. Sheft, and C. L. Chernick, ibid. 110 (1963).

20. H. H. Claasen, C. L. Chernick, and J. G. Malm, Noble-Gas Compounds, University of Chicago Press, Chicago, Ill., 1963, p. 287.

21. Gerhard Herzberg, Molecular Spectra and Molecular Structure. I. Spectra of Diatomic Molecules, 2nd. ed., (D. Van Nostrand Company, Inc., New York, 1950).

22. D. Andrychuk, J. Chem. Phys. 18, 233 (1950).

23. D. Andrychuk, Can. J. Phys. 29, 151 (1961).

24. D. F. Smith, Noble-Gas Compounds, University of Chicago Press, Chicago, Ill., 1963, p. 295.

25. J. R. Morton and W. E. Falconer, J. Chem. Phys. 39, 427 (1963).

26. J. L. Weeks and M. S. Matheson, Noble-Gas Compounds, University of Chicago Press, Chicago, Ill., 1963, p. 89.

27. W. E. Falconer and J. R. Morton, Proc. Chem. Soc., 95 (1963).

28. H. S. Johnston and R. Woolfolk, J. Chem. Phys. 41, 269-273 (1964).

29. D. J. Seery and Doyle Britton, J. Phys. Chem. (in press) (1966).

30. P. A. Agron, G. M. Begun, H. A. Levy, A. A. Mason, C. F. Jones, and D. F. Smith, Science 139, 842 (1963).

31. D. H. Templeton, A. Zalkin, J. D. Forrester, and S. M. Williamson, J. Am. Chem. Soc. 85, 242 (1963).

32. F. B. Dudley, G. L. Gard, and G. H. Cady, Noble-Gas Compounds, University of Chicago Press, Chicago, Ill., 1963, p. 61.

33. B. G. Baker and P. G. Fox, Nature 204, 466 (1964).

34. Synthetic Optical Crystals, Rev. ed. (The Harshaw Chemical Co., Cleveland 6, Ohio, 1955).

35. Parker O-Ring Handbook, Catalog 5700 (Parker Seal Company, Culver City, Calif., 1962).

36. Grating Monochromator Reference Manual Catalog Numbers 33-86-25 and 33-86-53, (Bausch & Lomb Incorporated, Rochester, New York).

37. Phototubes and Photocells, Technical Manual PT-60 (Radio Corporation of America, Lancaster, Pennsylvania, 1963), p. 113.

38. Gerhard Herzberg, Atomic Spectra and Atomic Structure (Dover Publications, Inc., New York, 1944), p. 202.

39. Phototubes and Photocells, Technical Manual PT-60 (Radio Corporation of America, Lancaster, Pennsylvania, 1963), pp. 95, 96, 185.

40. Kel-F Halofluorocarbon Oils, Waxes, Greases, and Alkanes, (Minnesota Mining and Manufacturing Company, Saint Paul, Minnesota, 1958).

41. Matheson Gas Catalog Number 25 (Matheson Company, Inc., Newark, California, 1965).

42. Matheson Fluorine Data Sheet (Matheson Company, Inc., Newark, California, 1965).

43. Terrell L. Hill, An Introduction to Statistical Thermodynamics (Addison-Wesley Publishing Company, Inc., Reading, Massachusetts, 1960), p. 83.

44. R. N. Doescher, J. Chem. Phys. 20, 330 (1952).

45. C. J. Ballhausen and A. D. Liehr, Phys. Rev. 106, 1161 (1957).

46. S. H. Bauer and C. F. Aten, J. Chem. Phys. 39, 1253 (1963).

47. O. G. Holms and D. S. McClure, ibid. 25, 1686 (1957).

48. R. Engleman, Mol. Phys. 3, 48 (1960).

49. G. E. Gibson, O. K. Rice and N. S. Bayliss, Phys. Rev. 44, 193 (1933).

50. T. A. Jacobs and R. R. Giedt, J. Chem. Phys. 39, 749 (1963).

51. P. Sulzer and K. Wieland, Helvet. Phys. Acta 25, (6), 653 (1952).

52. Roger L. Wilkins, J. Quant. Spectrosc. Radiat. Transfer. 4, (1964).

53. This is a joint effort of graduate students C. F. Weaver and Philip Dow under the direction of Professor H. S. Johnston.

54. S. W. Benson, The Foundations of Chemical Kinetics (McGraw-Hill Book Company, Inc., New York, 1960), p. 427.

55. Ph.D. Thesis of David James Wilson, California Institute of Technology, 1958.

56. R. G. W. Norrish, J. Chem. Soc. 3006 (1923).

57. G. C. Bond, Catalysis by Metals (Academic Press Inc., New York, 1962), pp. 70,130.

58. R. H. Griffith and J. D. F. Marsh, Contact Catalysis (Oxford University Press, London, 1957), pp. 100,254.

59. P. G. Ashmore, Catalysis and Inhibition of Chemical Reactions (Butterworths, London, 1963), pp. 112, 151,177,363.

This report was prepared as an account of Government sponsored work. Neither the United States, nor the Commission, nor any person acting on behalf of the Commission:

A. Makes any warranty or representation, expressed or implied, with respect to the accuracy, completeness, or usefulness of the information contained in this report, or that the use of any information, apparatus, method, or process disclosed in this report may not infringe privately owned rights; or

B. Assumes any liabilities with respect to the use of, or for damages resulting from the use of any information, apparatus, method, or process disclosed in this report.

As used in the above, "person acting on behalf of the Commission" includes any employee or contractor of the Commission, or employee of such contractor, to the extent that such employee or contractor of the Commission, or employee of such contractor prepares, disseminates, or provides access to, any information pursuant to his employment or contract with the Commission, or his employment with such contractor.